



“Flexible, Graphene-based Detector Arrays for Petrochemical Exposure Monitoring”

SBIR Phase I - Final Progress Report
Period of Performance: 09/01/2016 – 02/28/2017
Contractor: Seacoast Science, Inc.
Grant Number: 1R43OH010881-01A1

NATIONAL INSTITUTE FOR OCCUPATIONAL SAFETY AND HEALTH (NIOSH)
PA-14-071, NIOSH topic 14: “Exposure Assessment Methods for High Risk Occupations”

PI: Sanjay V. Patel
2151 Las Palmas, Suite C
Carlsbad, CA 92011

sanjay@seacoastscience.com
Ph# (760) 268-0083 x15
Fax# (760) 268-0662

Final Report Date: 5/9/2017

Table of Contents

Terms and Abbreviations	3
Final Report Abstract:	4
Section 1	5
1.1 Significant or Key Findings	5
1.2 Translation of Findings	5
1.3 Research Outcomes/Impact.....	6
Section 2 Scientific Report	7
2.1 Project Background.....	7
2.2 Specific Aims and Phase I Objectives	8
2.3 Experimental Methodology.....	9
2.4 Results and Discussion	12
2.5 Conclusion and Summary	31
Publications.....	33
Cumulative Inclusion Enrollment Table:	33
Inclusion of gender and minority study subjects	33
Inclusion of Children.	33
Materials available for other investigators.....	33
Bibliography & References Cited.....	34

Terms and Abbreviations

DPPZ	Diphenoxy phosphazene
DSC	Differential scanning calorimetry
ESD	Electrostatic discharge
fGNP	functionalized graphene nanoplatelet
GR	Graphene
LOD	Limit of detection
LEL	Lower explosive limit
PCP	Polycaprolactone
PECH	Polyepichlorohydrin
PEEK	Polyether etherketone
PEVA18%	Poly(ethylene co-vinyl acetate) 18% vinyl acetate
PIB	Polyisobutylene
PNC	Polymer nanocomposite
PPM	parts per million
PVA88%	Polyvinylalcohol 88% hydrolyzed
PVP	Polyvinyl pyrrolidone
R ₀ ,	Baseline resistance
ΔR	Delta resistance or sensor response
RH	Relative humidity
SBIR	Small Business Innovation Research
SEM	Scanning electron microscope(y)
TCE	Trichloroethylene
T _g	Glass transition point
T _m	Melting point

Title: Flexible, Graphene-based Detector Arrays for Petrochemical Exposure Monitoring

Investigator: Sanjay V. Patel, Seacoast Science, Inc., Carlsbad, CA 92011, (Email: sanjay@seacoastscience.com)

Affiliation: Seacoast Science, Inc.

State: CA

Telephone: 760 268-0083

Award Number: 1R43OH010881-01A1

Start & End Dates: 9/1/2016 – 2/28/2017

Program Area: Occupational Health

Final Report Abstract:

In Phase I of this SBIR program, Seacoast Science investigated the feasibility developing chemical vapor sensitive threads from a polymer-nanocomposite using the highly conduct nature of graphene and the selectivity of certain polymers toward specific chemical targets. Seacoast focused on determining what physical and chemical characteristics of these nanocomposites could be used to detect fuel-related hydrocarbons, specifically benzene and naphthalene, while excluding less noxious chemical vapors. The goal is developing an exposure monitor for workers who are commonly exposed to these chemicals. The ideal result of the project is a low-cost, easy-to-use, wearable chemical dosimeter in the form of threads sewn into badges or Velcro patches, that can be worn during work-shifts to log exposures in real time and simultaneously or subsequently transmit data.

Phase I focused on the determining what characteristics of polymers are necessary to fabricate robust sensing threads, and how to best process these threads for optimal sensitivity and durability. We used polymers that Seacoast has previously shown to have good sensitivity to hydrocarbons, particularly benzene. We included other selected polymers that can be used in conjunction with pattern recognition techniques (in Phase II) for interferent rejection.

To fabricate the threads, Seacoast employed common manufacturing techniques, including solution-extrusion, melt-extrusion, and solution-casting methods. Thread materials were exposed to vapors of 10 different chemicals to compare response characteristics. The Phase I work showed that the method of fabrication highly influenced both the sensitivity of the threads as well as physical properties of the threads. Early in Phase I, we discovered that the temperatures required for melt-extrusion were sufficiently high as to destroy the chemical sensing properties of the majority of the polymers. Based on this finding, the fabrication strategy and the work plan were modified. Because melt temperatures degraded the polymers, solution-extruded threads had better sensing characteristics than melt-extruded threads. Additionally, melt-extruded threads were very fragile, which is a concern that needs to be addressed before field-use of this technology will be practical. In contrast, solution-cast and solution-extruded threads had comparable sensitivity and both had better sensitivity than melt-extruded threads. Both were stronger than melt-extruded threads, but their thickness is more difficult to control when fabricating devices in small prototype quantities. In addition, a thermal annealing treatment markedly reduced signal-noise for one of the key benzene and naphthalene sensitive polymer-nanocomposites, vastly improving sensitivity for this application.

In Phase II the materials will be optimized and a fully integrated readout system will be developed. Mechanical properties will be studied to improve ruggedness for field-use. These systems will be tested in Seacoast's controlled test room, on mannequins, to simulate various exposure conditions, and verify system performance. Algorithms to compensate for environmental factors will be developed and implemented in a robust electronics package.

Section 1

1.1 Significant or Key Findings

The objective of this work is to develop a wearable, lightweight, exposure monitor for workers handling hydrocarbon fuels and fuel-related compounds.

The sensing technology combines graphene as a conductive dopant with chemoselective polymers to form polymer-nanocomposites (PNCs) as a new class of resistive chemical sensors. PNC chemiresistors^{1,2,3} preferentially absorb target fuel vapors causing the PNC's to swell.⁴ The graphene in the PNC's imparts measurable electrical conductivity to the composite materials. We previously demonstrated^{5,6} the use of graphene in selective chemiresistors, and showed that an order-of-magnitude less graphene could be used to create chemiresistors with similar sensitivity and performance to chemiresistors made with graphite or carbon nanotubes. We hypothesize that the reduced dopant concentration leads to stronger, more sensitive chemiresistors.

Phase I focused on the determining what characteristics of polymers provided physically robust, chemical sensing threads, and how to best process the starting materials to obtain the desired form of a physical thread. We used polymers that we have shown to be sensitive to hydrocarbons, including benzene and fuel-related targets, as well as other polymers shown to be useful for pattern recognition techniques for interferent rejection. Seacoast compared common thread manufacturing techniques (solution-extrusion and melt-extrusion) and solution-casting methods. Extruded and cast materials were exposed to vapors of 10 different chemicals in a vapor test system to compare response characteristics. These sensors respond reversibly to chemical vapors, with their resistance increasing to varying degrees, and returning to baseline in clean air. Thus, the sensors are reusable, and total exposures can be measure by continuous integration of the resistance change over time.

An applied research finding of this Phase I project was that the method of fabrication highly influenced the sensitivity, and physical properties of the chemical sensitive threads. Early in Phase I we determined that the temperatures required for melt-extrusion degraded the chemical sensing properties of most of the polymers proposed for this application. This necessitated a refocusing of the proposed fabrication strategy and work plan. Solution-extruded threads had better sensing characteristics than those that were melt-extruded. However, the fragility of these threads is a concern that needs to be overcome. In contrast, solution-cast materials had comparable performance to the solution-extruded materials, and were stronger, but their thickness is more difficult to control when fabricating devices in small prototype quantities. Nonetheless, these types of materials were found to be compatible with sewing into conductive fabric templates, which ultimately can be made into the proposed chemical sensing patches.

A basic research finding of this project was a thermal treatment reduce sensor noise, and increase response speed and sensitivity, thereby improving limits of detection (LOD's). The effects of this treatment were explored in detail using chemical exposure data, and samples of treated threads were submitted for differential scanning calorimetry (DSC) to better quantify physical and chemical phenomena occurring during the thermal treatment. The DSC results match the observed changes in resistance, and indicate that the thermal treatment fundamentally changes the nanocomposite structure, allowing for the observed improvements in benzene vapor sensing performance. Further investigation and optimization of this effect is required to determine if this thermal treatment can be used with other PNC's for detecting other types of chemicals.

1.2 Translation of Findings

The findings in this work will lead to improvements in the fabrication of a novel type of wearable sensors and chemical dosimeters. The intent is to construct the dosimeters in the form of patches or badges, to provide a low-cost and light-weight alternative to bulky and expensive gas detectors currently

needed for dosage testing. These dosimeters will track worker exposure to potentially carcinogenic fuel vapors during the work-shift and allow for further analysis of data via wired or wireless transfer. Ultimately these threads could be sewn directly into smart clothing to warn and protect workers in many industrial settings.

1.3 Research Outcomes/Impact

This project is a first step to developing a new class of wearable chemical sensors, where the chemical sensing elements are fabricated in the form of threads rather than conventional electrical interconnections. Initial devices will be sewn as patches or light-weight badges, and will be disposable or recyclable. Ultimately the chemical sensing threads will be sewn directly into workers' uniforms or protective garments. Potential outcomes are direct temporal tracking of worker exposure to fuel-related chemicals that can be used for reducing long-term exposures, and improving occupational health.

The objective is development of a wearable fuel-exposure dosimeter, similar in scope to the inexpensive gamma radiation dosimeters used by nuclear power plant workers. Innovations that allow development of this innovative chemical dosimeter include: (1) low-cost, light-weight flexible electronic circuit substrates; (2) low-cost PNC chemiresistors tuned for high sensitivity; and (3) creation of sensing threads from these composites that can be woven into fabric patches. We also expect this project to be the first step to more complex wearable smart fabrics for other detection markets. Further outcomes can be achieved by tuning these devices for other chemical targets or industry specific targets, such as jet fuels, pesticides, or military exposure concerns.

This exposure monitor/dosimeter will be useful in a variety of workplaces for routine monitoring and will measure fuel exposures rapidly and inexpensively. In 2008, there were 161,600 workers in the U.S. oil & gas industry and a total of 717,000 workers in the U.S. mining industry.⁷ While there are sensors for lower explosive limits (LEL) and for tracking dangerous chemicals (CO, CO₂, H₂S), there is no low-cost product available to track worker exposure to ppm-levels of fuels.

Section 2 Scientific Report

2.1 Project Background

With massive growth of the U.S. oil and gas industries in recent years, which is anticipated to continue well into the future,^{8,9} many more workers are being and will likely face exposed to harmful levels of petrochemicals than ever before. Although crude oil and gas are buried deep underground, they are pushed to the surface under tremendous pressure, where they are processed, handled and transported by workers above ground, e.g. at refineries, airports, and fueling depots. The U.S. Bureau of Labor Statistics states regarding 2010, “exposure to harmful substances or environments,” accounted for 409 fatalities¹⁰ and a non-fatal injury incident rate of 5.2 injuries per 10,000 full time workers.¹¹ There were also 19,300 cases of non-fatal occupation-related illness¹² due to respiratory conditions, and 3,200 poisonings in the U.S.

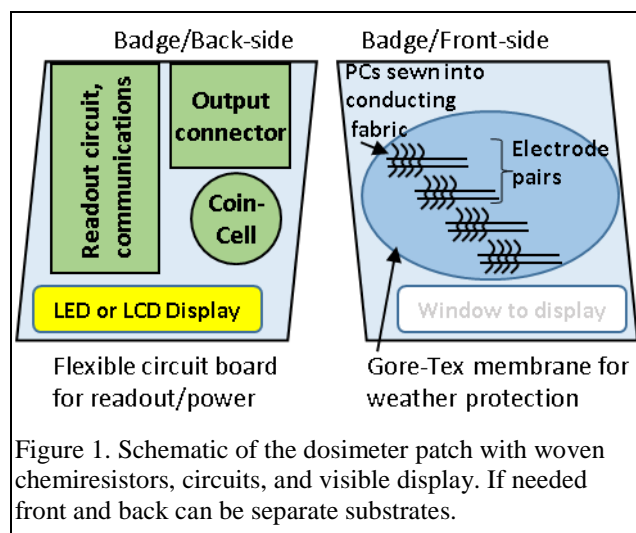
Commercial radiation dosimeters cost between \$50 (thermo-luminescent badge) and \$500 (with electronic readout). Aside from single gas monitors for CO, methane, or CO₂, no chemical sensor system exists in this price range (< \$100) to monitor workers’ exposure to hazardous chemicals. Dräger tubes are commonly used for exposure monitoring applications. Their color-change mechanism is easy to see, but difficult to quantify, and for petrochemical hydrocarbons (\$75 ea.¹³) they have many cross-sensitivities, including CO, lighter hydrocarbons, and perchloroethylene, and their sensitivity is limited to >10ppm.¹⁴ Dräger tubes for specific chemicals are available, but have poor selectivity.¹⁵ Electronic single-gas detectors cost¹⁶ from \$189 (Honeywell Gas Alert) to over \$1500 (Dräger X am), but none are specific to fuels or hydrocarbons. More specific detectors cost thousands of dollars and are typically not lightweight, wearable “hands-free” devices.

Price and quality represent significant barriers to adequate worker protection. Seacoast’s low-cost solution to the problem of chemical exposure assessment is a wearable dosimeter badge. Such badges are made from polymer-based detectors designed to be sensitive specifically to noxious chemical vapors encountered in the petrochemicals and related industries. The composite sensors, formed into threads, are to be woven into disposable badges or patches that are attached to readout electronics. The dosimeter badge will provide workers and regulators with data regarding daily exposures to vapors emitted during oil, gas, and biofuels processing.

Although chemiresistive sensors and other polymer-based sensors have been commercialized for several years, no one has effectively created a low-cost sensor system from this technology. We propose to capitalize on the unmet market space of low-cost chemical exposure dosimeters. Modern conductive fabrics and flexible circuit technologies make this possible, without requiring microchip substrates.

Innovation: The proposed product consists of 2 main parts, a front piece (potentially disposable) containing the detecting elements fabricated from PNC threads woven into a patch, and a backing containing the electronic readout and data-logging features on a light-weight circuit with a rechargeable coin-cell battery (Figure 1).

Workers will wear this patch during their normal shift, and then turn it in at the end of the day for data-download and long-term tracking. Ultimately, the intent is for the entire device, or perhaps, just the front badge component, can be discarded or recycled, and a new one affixed for the next day. The circuitry will measure the resistances of the sensing threads, and compensate for environmental variations and detected



interferents, to integrating the total exposure. The total exposure can be downloaded to a database as needed.

We anticipate different patches will be developed for civilian and military uses: thus, sensor badges can be sold for different classes of chemicals, i.e. gasoline, jet-fuels, pesticides, etc. The polymers are inexpensive, the PNC threads can be extruded or cast for <<\$1 per foot, and circuitry can be made for under \$20 (volumes of 1000's). Based on our preliminary prototypes (below) we estimate the product price can be under \$50 in volumes >1000.

Concept of Operations/Features:

- Conductivity of different threads changes upon exposure, reversibly, depending on concentration and chemical -- measured by electrical (direct current, DC) resistance.
- Eliminating the substrate support from the detector, and simply sewing the detector threads into a patch or fabric swatch has the benefits of being extremely low cost, making the detector elements disposable, eliminating the need for long-term recalibrations¹⁷ typically required due to wear-and-tear or aging.
- Simple onboard algorithms compensate for flexing, temperature, humidity, and other variables.
- Since the patch is worn outside of the wearer's own clothing or uniform, affixed by Velcro or other means, and the resistance measurement mechanism uses extremely low voltage and currents, the system is intrinsically safe, and cannot harm the wearer, thus meeting UL and CSA safety requirements.
- The detecting threads are themselves protected by liquid-resistant, vapor-permeable membrane (e.g. Gore-TEX) to allow operation in wet environments; the readout is encased in epoxy as is done commonly in the industry.

2.2 Specific Aims and Phase I Objectives

Workers in the petrochemical and biofuels related industries are regularly exposed to vapors from the chemicals they process or handle. Fuels are mixtures of many similar chemicals, and most fuels contain known carcinogens, such as benzene, yet no device exists to monitor worker vapor exposures to the hazardous vapors. Lack of sensor selectivity towards fuels or potentially carcinogenic fuel-components is the biggest developmental challenge. A further option would be to use exposures to certain marker compounds (e.g. C₅-C₈ hydrocarbons) to differentiate among fuel exposures.^{18,19} A fuel-dosimeter product must overcome barriers of cost, size, and weight.

In Phase I, Seacoast proposed a multi-detector array incorporated into a lightweight badge for measuring gasoline vapor exposures. This badge could be worn (clipped or velcro'ed) on the outer-most layer of clothing or protective suit, allowing workers to monitor their cumulative exposure. A rechargeable coin-cell battery will provide power and a USB connection will both recharge and allow data transfer. Once this concept is proven on a fabric support, there is potential to take the next step of weaving the sensor threads directly into industrial chem-suits, and other protective garments at the time of manufacturing, thereby creating smart clothing. Mass-production fabrication methods can make the sensors inexpensive. We will use our multidisciplinary expertise in polymers and in low-cost circuitry design and fabrication to design chemical sensing patches that are sufficiently small and lightweight so as not to reduce worker mobility.

From this work, we expect to answer several scientific and engineering questions:

1. Which chemoselective absorbent polymers can be formed into threads that provide the sensitivity and selectivity necessary for fuel exposure monitoring?
2. How can reproducible, robust threads be fabricated in high volumes?

3. Do graphene composites improve the robustness, sensitivity, and/or selectivity of the threads over other allotropes?
4. How can an array of chemisorbent threads be protected from environmental degradation while providing compensation for the various physical, electrical and environmental variables that workers experience during normal duty?

Specific Aim 1) Select materials for the dosimeter array that can be used for selective and sensitive detection of chemicals indicative of fuel exposure.

Milestone 1: (1a) Initial polymer selection, determine graphene content for viable sensors, test against targets and interferents at various concentrations at different temperature and humidity levels; and (1b) Extruded threads tested against target chemicals and environmental variables.

Metrics: (a) Polymer-graphene composites demonstrated in lab to be sensitive to 10% of NIOSH reference exposure levels; and (b) optimal polymers selected for thread manufacturing development; (c) extruded threads tested for sensitivity and performance.

Specific Aim 2) Demonstrate low-cost volume manufacturing path using commercial micro-extrusion.

Milestone 2: Working with Randcastle, fabricate thread samples using micro-extruder. Determine which materials can be extruded and how to incorporate graphene into the composites.

Metrics: (a) Array of threads fabricated, and (b) preliminary recipes established.

Specific Aim 3) Determine effects of environmental and physical variables on the threads/arrays.

Milestone 3: Threads and electronics tested against electrostatic discharge (ESD), bending, temperature, humidity to determine the effect of these variables, and need for compensation and physical or electrical protection of the device.

Metrics: (a) Algorithms developed for compensating for temperature and humidity; and (b) designs developed for compensating for ESD and bending.

2.3 Experimental Methodology

In Phase 1, Seacoast focused on ways to make uniform threads from several types of polymers and graphene; evaluated different grades of graphene and functionalized graphenes; investigated how to integrate or modify polymers which may have poor physical properties but good sorbent properties into stand-alone threads; and tested the threads for their sensing capabilities with different chemical targets and potential interferences.

Polymers: Phase I polymers (Table 1) were limited to materials that have been shown^{1,4,5} to be well suited for chemiresistors, i.e. they are solid at room temperature, soluble in common solvents, and readily mixed with graphene to form PNCs. In Phase II we will expand the diversity of the polymers to achieve better sensitivity and fill in gaps in the array. The polymers were selected for their diversity, and for their known capacity to absorb fuel-related target chemicals (Table 2) and potential interferents in the petrochemical industries. For example, some targets (*i*-pentane, *i*-octane) are used in the remediation industry to track underground sources of groundwater pollution from leaky gas station fuel storage tanks.¹⁸

Table 1. Phase I Polymers and Selection Rationale

Polymer	Properties	Rationale / Peak sensitivity	T _m or T _g (°C)
Polyisobutylene (PIB)	Nonpolar polymer	Peak: Cyclohexane – Xylene; Highest sensitivity to lowest polarity chemicals ¹ with $\delta \leq 18$	T _g = -64
Polyethylene (co-) vinylacetate (PEVA) (18% acetate)	Low Polarity, low-crystallinity polymer	Peak: Trichloroethylene (TCE); Highest sensitivity to Low-mid polarity ¹	T _m = 88
Diphenoxy phosphazene (DPPZ)	Mid-polarity, rubbery polymer	Peak: THF, Chloroform; Highest sensitivity to solvents ⁴ with $\delta \approx 20 \text{ MPa}^{1/2}$	T _g ²⁰ = -10
Polypichlorohydrin (PECH)	Mid-polarity, hydrogen bond-base	Demonstrated response to toxic industrial chemicals ²¹ and chlorinated solvents ²²	T _g = -22
Polycaprolactone (PCP)	Mid polarity, low hydrogen bonding.	Demonstrated high sensitivity ²³ to mid-range polarity chemicals; $\delta^{24} \sim 21 - 21.85$	T _m = 60 T _g = -60
Polyvinyl pyrrolidone (PVP)	High polarity, strong hydrogen bonding	Peak: Ethanol, Methanol – Water; High sensitivity to polar hydrogen bonding chemicals ¹	T _g = 150-180
Polyvinyl alcohol (PVA)	High polarity, strong hydrogen bonding	Peak: Methanol; High sensitivity polar hydrogen bonding chemicals ⁴	T _g = 80

Target analytes: ACS-grade isopentane, isooctane, benzene, toluene, naphthalene, trichloroethylene, acetone, ethanol, methanol, were purchased from Sigma Aldrich and used as received. Naphthalene was not one of the test chemicals listed in the original proposal, but was added because of its prevalence in jet fuels, and importance to the military and airline markets. Deionized water was sourced from an in-house system. Lab air was sourced from an in-house oil-less air compressor; air was passed through Drierite for use as the carrier gas for all tests.

Table 2. Phase I Target Chemicals, Properties,⁴ and NIOSH Worker Safety Limits²⁵

Target	Chemicals	HSP (MPa ^{1/2})	15min STEL (ppm)	8-hr TWA (ppm)	Selection Rationale
Petrochem. component	Isopentane	13.7	610 (pentanes)	120	Major component in fresh gasoline ^{18,19}
	Isooctane	14.1	385 (octanes)	75	Major component in weathered gasoline ^{18,19}
	Benzene	18.5	1	0.1	Component in fuels, ^{18,19} carcinogen
	Toluene	18.16	150	100	Component in fuels ^{18,19} , and Shale oil ²⁶
	Naphthalene	20.2	15	10	Common component in Jet fuels ²⁷
Interferent	Trichloroethylene (TCE)	18.7	Goal: detect the petrochemical fuel component in a background of 100 ppm of the interferent chemicals, and up to 80% relative humidity.		Degreasing solvent, common industrial interferent
	Acetone	19.9			Common solvent and interferent
	Ethanol	26.5			Common solvent, biofuel additive, food industry
	Methanol	29.6			Common solvent, used for airplane deicing
	Water	47.8			Most common interferent

Conductive carbons: Five grades of unfunctionalized, pristine graphenes were tested. Graphene powder (N002-PDR) was purchased from Angstrom Materials²⁸ (Dayton, OH), whereas the other types were from Graphene Supermarket²⁹ (owned by Graphene Laboratories Inc., Calverton, NY). Functionalized graphene nanoplatelets (fGNPs) were also purchased from Graphene Supermarket. All carbon materials were used as received without further purification. The fGNPs were functionalized using the Haydale plasma process³⁰ (HDPlas®) (Table 3).

Table 3. Carbon Allotropes used for Phase I Chemiresistors

Material; specified dimensions	Source Part #	Surface Area (as specified), m ² /g
Pristine Graphenes (GR):		
GR; Thickness (average) < 3 graphene layers, x-y ≤ 10 μm	N002-PDR	400 - 800
C1 (GR-C1); Thickness = 5-30 nm, x-y ~ 5-25 μm	Grade C1	80
AO-2 (GR-AO2); Thickness = 8nm (20-30 monolayers), x-y ~0.15-3μm	Grade AO-2	100
AO-3 (GR-AO3); Thickness = 12nm (30-50 monolayers), x-y ~1.5-10μm	Grade AO-3	80
Graphene AO-4 (GR-AO3); Thickness = 60nm, x-y ~ 3 -7 μm	Grade AO-4	< 15
Functionalized Graphene Nanoplatelets (fGNP):		
fGNP-Argon; Thickness <50nm, x-y ~ 0.3 -5μm	AR-HDPLAS-5G	~20
fGNP-Carboxyl; Thickness <50nm, x-y ~ 0.3 -5μm	COOH-HDPLAS-5G	~20
fGNP-Fluorocarbon; Thickness <50nm, x-y ~ 0.3 -5μm	F-HDPLAS-5G	~20
fGNP-Ammonia; Thickness <50nm, x-y ~ 0.3 -5μm	NH ₃ -HDPLAS-5G	~20
fGNP-Nitrogen; Thickness <50nm, x-y ~ 0.3 -5μm	N-HDPLAS-5G	~20
fGNP-Oxygen; Thickness <50nm, x-y ~ 0.3 -5μm	O ₂ -HDPLAS-5G	~20

Chemical, humidity, and thermal testing: Seacoast has several custom-built vapor testing stations (VTS, see Facilities and Equipment) that allow stringent testing of sensors over the entire industrial temperature scale, at all levels of relative humidity (RH), and at time scales ranging from seconds to months. Seacoast's test systems each have a 20-channel, electrical-resistance measuring datalogger (Agilent, Inc.), with which we can test 20 chemiresistors in parallel. Using one test station, we tested (measure resistance in response to chemical exposure or other variable) both bare threads and threads woven into a representative patch. Thermal anneals (up to 60°C) could be done in the same test system prior to the vapor challenges, allowing control of the air environment during the thermal treatments. Annealing at temperature >60°C were done in a Test Equity (105A) environmental chamber, capable of reaching 130°C, without control of the humidity. Due to the limited amount of time in Phase I and the many variables (types of polymers, conductive materials, chemicals) the sensor tests were streamlined to a small set of vapor challenges, to allow for rapid screening of devices. More extensive testing is proposed for Phase II.

Polymer-graphene suspensions: In this work, sensor materials were fabricated using three methods: solution casting, melt-extrusion or solution-extrusion. Before fabrication as threads, the polymer was dissolved in a compatible solvent, followed by addition of graphene nanoplatelets until the final desired concentration of solids was achieved, usually 1% - 15% by weight. These suspensions were then sonicated for up to 3 hours prior to use.

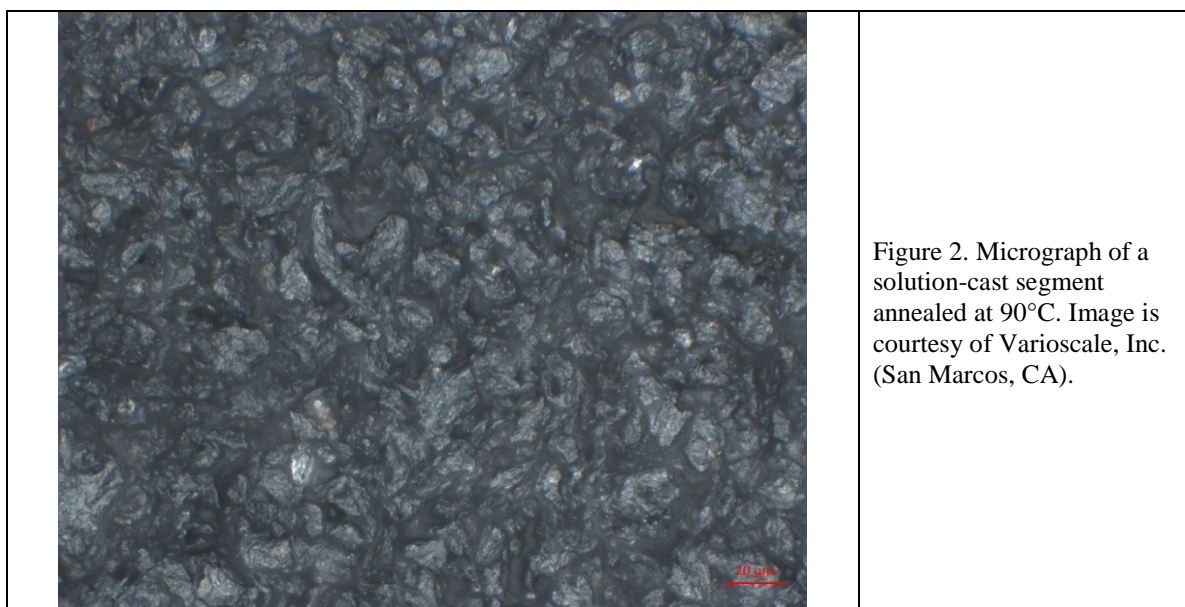
Solution Casting: Casting solutions evaluated in this project, were 1-5 wt. % solids, which allowed them to flow into molds or over the deposition substrate freely. Solution-cast materials were formed by pouring the suspension into a glass Petri dish, or using a syringe to cast a film on to a microscope slide, and allowed to air dry at room temperature. Segments were then cut using a razor blade and attached to the forked pin rails using silver paste. Alternatively, some threads were formed by depositing the solutions into a mold cut into a polyether ether ketone (PEEK) substrate.

Extrusions: Melt-extruded threads were formed by: Casting the suspension into a petri dish; Allowing the material to solidify; placing segments of the cast film into a custom aluminum syringe; heating the syringe to 150°C; and extruding the threads through an 18-gauge needle, cut to ~1/4" to reduce the dead volume, onto a room temperature microscope slide. The resulting melt-extruded threads were visibly denser than the solution extruded threads, but had significant noise and low responses.

Solution-extruded threads were formed by forcing the polymer-graphene suspensions through a standard glass 10ml syringe and stainless steel needle, cut to ~1/4" to reduce the dead volume. These solutions were typically >15 wt. % solids to achieve sufficient viscosity for the extruded threads to retain their shape. The 15 wt. % solutions were used as the stock material; greater densities were obtained by

allowing solvent to evaporate from these stock solutions. Standard 18 and 22 gauge needles were used as nozzles to extrude the chemiresistor threads for which data are shown here. Finer gauge needles produced threads that were too fragile to handle. The threads were extruded at room temperature onto a microscope slide for support and allowed to dry prior to cementing segments of the threads to the forked pins for testing.

The differing fabrication techniques produced threads of varying morphologies that were optically distinct under low-magnification optical microscopy. Extruded threads had the appearance of foam insulation with extensive void spaces visible on the surface. Cast materials had a denser, smoother appearance (Figure 2). Cast segments had lower starting resistance values than the extruded threads. In addition, cast segments were somewhat thicker, more rigid, and less fragile than the solution-extruded threads.



Mechanical strain tests: For strain tests, threads were sewn into conductive fabric samples, and a strain gauge³¹ was attached to the back of this “patch” using double sided tape. The strain gauge (nominal resistance 120Ω) was connected to a Wheatstone bridge to allow higher resolution measurement of the applied strain. The resistance of the thread was simultaneously measured with a data logger to correlate the resistance changes to strain.

2.4 Results and Discussion

Specific Aim 1) Select materials for the dosimeter array that can be used for selective and sensitive detection of chemicals indicative of fuel exposure.

Milestone 1:	
1a) Initial polymer selection, determine graphene content for viable sensors, test against targets and interferences at various concentrations at different temperature and humidity levels; and	√
1b) Extruded threads tested against target chemicals and environmental variables.	√
Metrics:	
(a) Polymer-graphene composites demonstrated in lab to be sensitive to 10% of NIOSH reference exposure levels;	√
(b) optimal polymers selected for thread manufacturing development;	√
(c) extruded threads tested for sensitivity and performance.	√

Task 1) Materials Development and Testing:

In this work, we were only able to fully explore a few of the many variables that are available to manipulate to achieve the desired behavior of polymer-nanocomposite sensors. Variables investigated to date are noted in Table 4.

Table 4. Physical, chemical and process variables important to developing nanocomposite-thread based chemical sensors.

Variable	Phase I Status
Polymer composition	
• Functionalization and chemical composition	Limited investigation of 7 materials
• Molecular weight	Planned for Phase II
Type of graphene	
• Including source/vendor • Particle size • Functionality, if any	Limited study, further optimization required in Phase II.
Fabrication method	
• Solution-casting	In depth study in Phase I
○ Using a mold, ○ Free standing, ○ Spin-casting, ○ Substrate and substrate temperature, ○ Film thickness	In depth study in Phase I, In depth study in Phase I, In depth study completed prior to Phase I, None, Limited study performed, further study required in Phase II
• Solution-extrusion	In depth study in Phase I
○ Solution density, ○ Relative amount of polymer to graphene, ○ Solution temperature, ○ Solvent type, ○ Thread size (die or syringe size)	In depth study in Phase I, optimized formulation of select polymers developed; In depth study in Phase I, None, None, 3 gauges tested, further optimization required
• Melt-extrusion	
○ Relative amount of polymer to graphene, ○ Extruder temperature, ○ Thread size (die or syringe size), ○ Substrate temperature	Limited study performed, Limited study performed, Limited study performed, Limited study performed
Post-processing	
• Vapor treatment, • Thermal treatment (anneal)	Limited testing in toluene, In depth study in Phase I, optimized formulation of select polymers developed. Further optimization required for other polymers

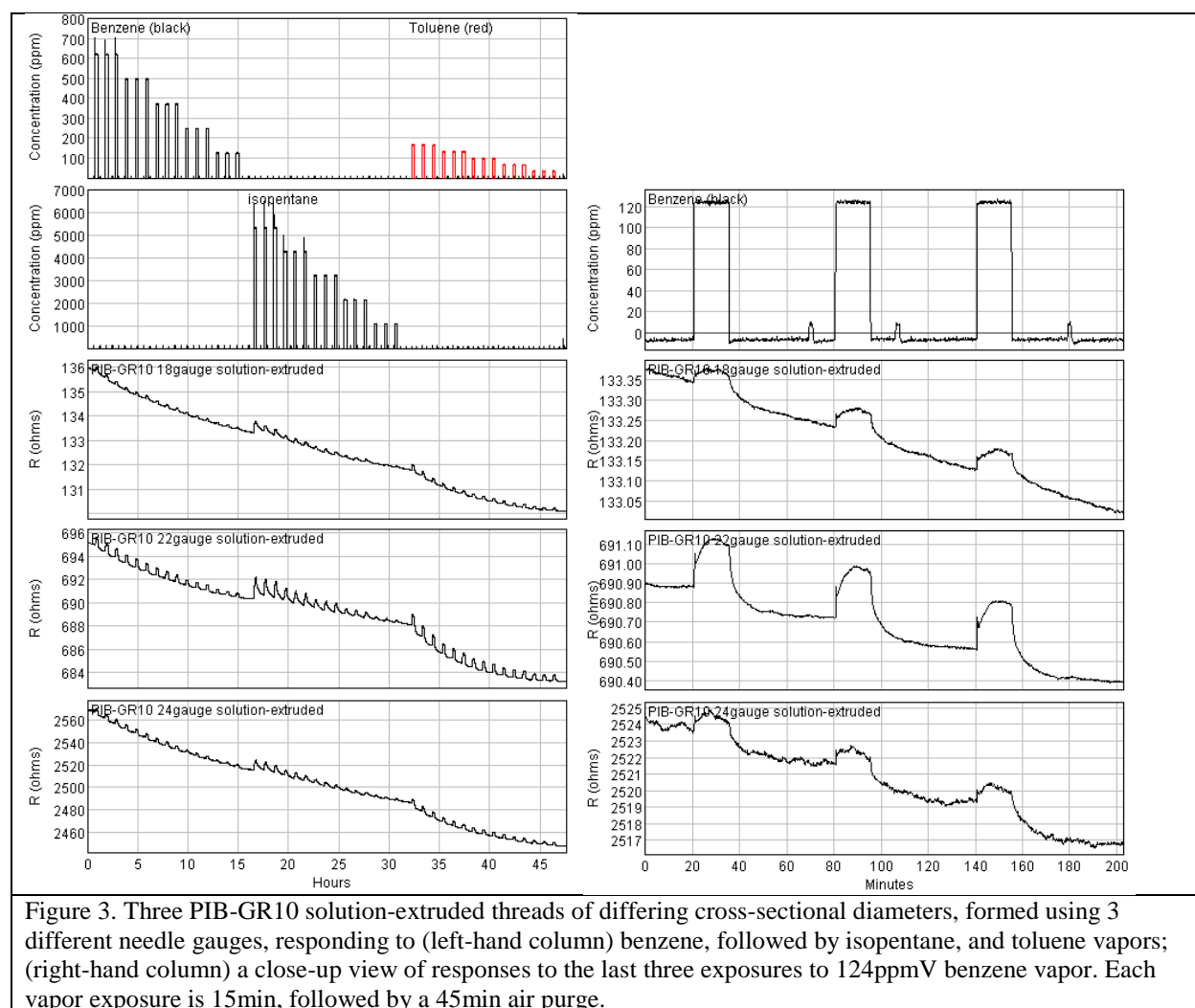
Starting with PEVA18%, as a “control” polymer, early work focused on identifying a candidate graphene material that we would use to focus our further development. Some of this work was done on our prototyping platform, which allows rapid fabrication and comparison of different materials, having 9 gold plated electrode pairs in a small size compatible with the test station configuration. We evaluated several types of both functionalized and unfunctionalized (pristine) graphenes, at varied ratios with PEVA18.

Previously,⁵ we used solution drop-casting onto silicon wafers to produce a polymer film that was subsequently dissected to mimic a polymer thread. The thickness of the individual PNC threads was not constant, contributing to sensor-to-sensor variations. In this work, we looked to improve

manufacturability to improve reproducible resistance of the finished threads. In addition, we modified existing formulations to optimize the graphene to polymer ratio to increase sensitivity to target vapors.

Comparing Polymers: The survey of polymer materials proposed for the Phase I project, was as much to determine what properties were useful for making viable threads, as to study their vapor sensitivity. Of the proposed polymers, polyvinyl pyrrolidone (PVP) and diphenoxy phosphazine (DPPZ), when mixed with the graphene, could not be formed into threads successfully. These polymers, when cast as solutions were too brittle to be used as a free-standing thread. This does not preclude future use of these polymers in melt-extruded PNCs; however, Phase I is too brief to complete further testing with these polymers.

Figure 3 shows the responses of PIB-GR10 solution-extruded threads, of differing diameters, fabricated through 18-gauge (0.84mm inner diameter (ID)), 22-gauge (0.41mm ID), and 24-gauge (0.31mm ID) needles. PIB is a very common rubbery non-polar polymer (the basic compound in butyl rubber). The electrical resistance of the threads increases when exposed to each vapor, and return, reversibly, to baseline when exposed to clean air.



LOD's³² from these PIB solution-extruded threads for benzene, isopentane, and toluene are shown in Table 5.

Table 5. Limits of detection (ppm) from PIB-GR10 solution-extruded threads

Chemical (exposure)	18-gauge	22-gauge	24-gauge
Benzene (124ppm)	30 ppm \pm 15 ppm	5 \pm 0.2	51 \pm 17
Isopentane (1055ppm)	247 \pm 172	40 \pm 4	152 \pm 21
Toluene (33ppm)	3 \pm 0.3	0.6 \pm 0.01	3 \pm 0.5
Isooctane (301ppm)	No Data	3 \pm 1	14 \pm 6

The ultimate Phase I goal is to detect 10% of the 15-min STEL and 8-hr TWA of the “petrochemical component” targets in Table 2. The data in Table 1 show that for toluene, isooctane, and isopentane, the detection limits are below the 10% benchmark for the 8-hr TWA (120, 75, and 100 ppm respectively). For benzene, the LOD from the 22-gauge thread, 5ppm, is equal to the current OSHA short-term regulation (5ppm), but not as low as the NIOSH guidelines.

Figure 4 shows a benzene test set, using PCP-GR10 solution extruded threads, from three different needle sizes. The LODs from these sensors was 15 \pm 2ppm, 13 \pm 1ppm, and 14 \pm 1ppm, from the 18-, 22-, and 24-gauge needles, respectively.

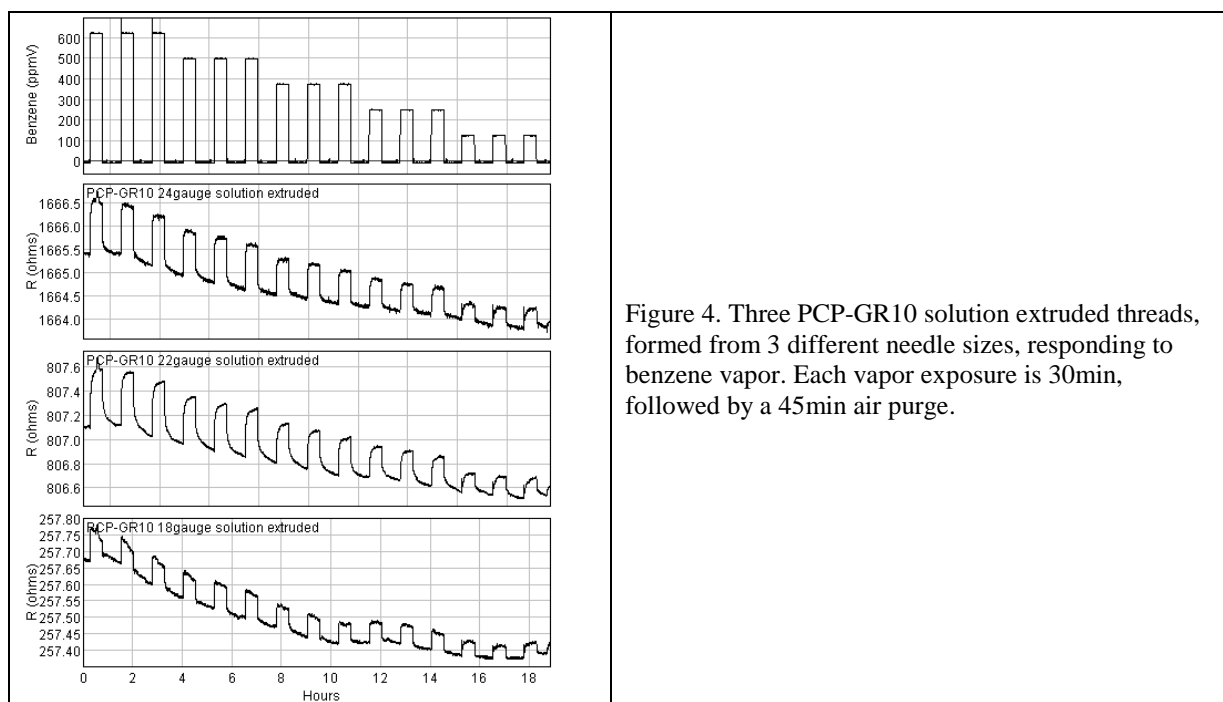
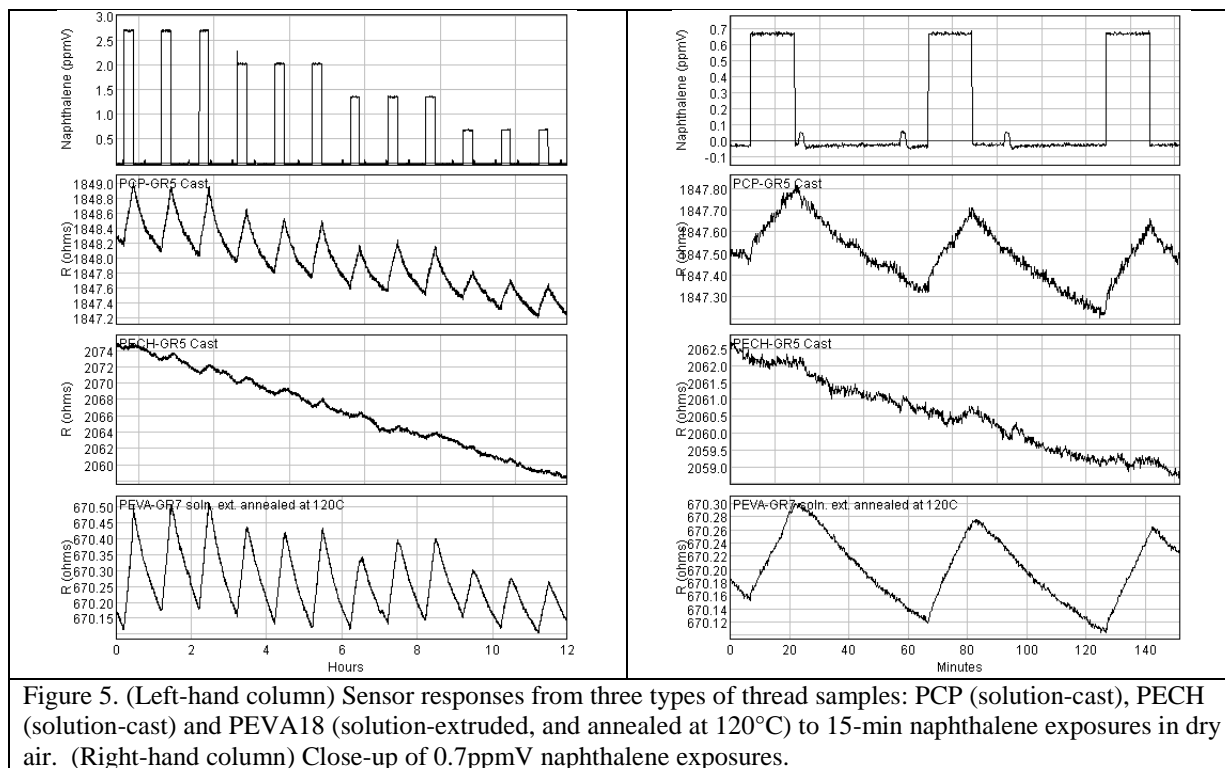


Figure 4. Three PCP-GR10 solution extruded threads, formed from 3 different needle sizes, responding to benzene vapor. Each vapor exposure is 30min, followed by a 45min air purge.

Figure 5 shows a comparison of three types of threads when exposed to naphthalene vapor. The naphthalene exposures resulted in slow, but reversible, resistance increases, which is to be expected from large molecules that diffuse very slowly into and out of polymers.

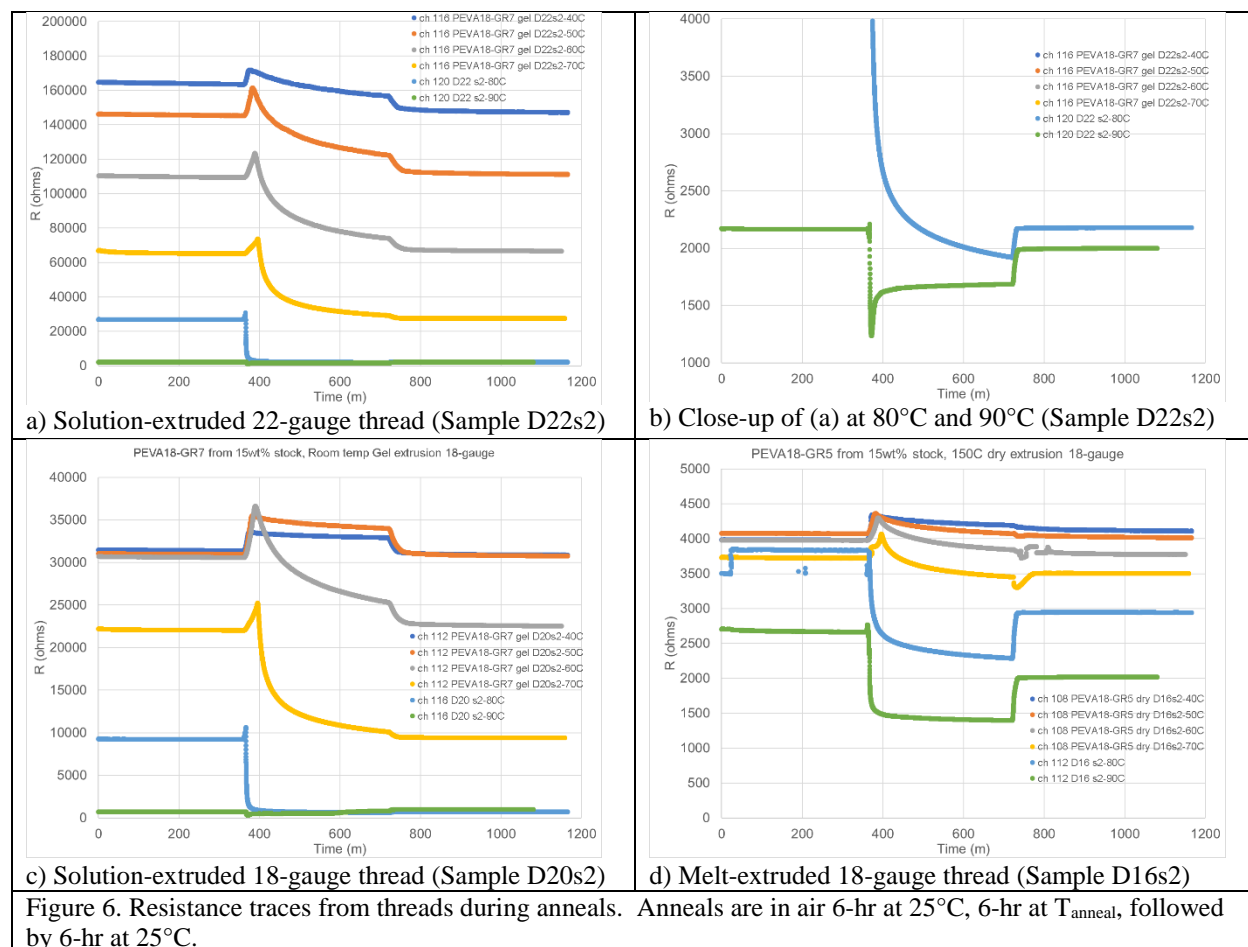


From these data, naphthalene limits of detection from the 15-min peak responses from the PCP, PECH, and PEVA sensors, are: 0.1 ± 0.02 ppm, 0.9 ± 0.3 ppm, and 0.06 ± 0.01 ppm, respectively. These are all well below 10% of the NIOSH short-term and 8-hr guidelines. The LOD from the PEVA-GR7 thread was 13 ± 3 ppm.

We observed that different polymers require different concentrations of the same type of graphene to produce responsive threads, suggesting that the arrangement of the graphene plays a role in the structure of the final material.

Focus on improving sensitivity: From initial tests, benzene was the most difficult chemical target to detect at below the NIOSH guidelines. We hypothesized that annealing the threads would help to relieve stress in the sensors and help stabilize the sensors at higher temperatures. Therefore, we focused on improving the chemiresistors for benzene, and specifically looked at thermal treatments to try to improve baseline stability (reducing drift) and sensor reproducibility. PEVA-GR was selected as the main focus for this work to reduce the number of variables.

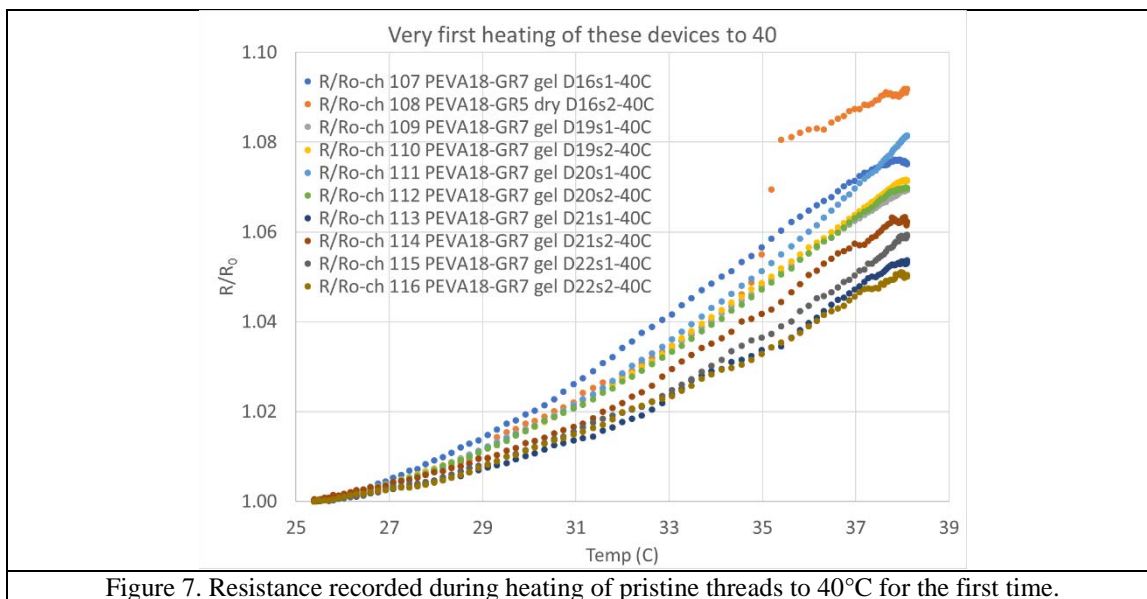
Several PEVA-GR samples were annealed in 10°C increments and tested against benzene vapors between anneals. Figure 6 shows the resistance of three samples recorded during the anneals (D22 = 22-gauge solution-extruded; D20 = 18-gauge solution-extruded; D16 = 18-gauge melt-extruded).



The major changes in the solution-extruded threads occur during the anneals at 50°, 60°, 70° and 80°C. During initial heating, the resistance is seen to increase then decrease in all cases. When held at elevated temperature during the 6-hr treatment, the resistance of all the threads is seen to decrease. A close-up of the 80°C and 90°C anneals shows that the resistance change before and after the 90°C anneal is much smaller than at any lower temperature. From the initial pristine samples to the post-90°C annealed state, the baseline resistance (R_0 in 25°C, dry air) dropped a factor, X ($X = R_{\text{pristine}}/R_{\text{post-90}^\circ\text{C}}$) equal to 35 ± 22 and 90 ± 12 , for the 18-gauge and 22-gauge solution-extruded threads respectively. In contrast the R_0 for the melt-extruded threads (Figure 6b) dropped only a factor of 2, suggesting that the structure was mostly set during extrusion.

Another effect of the anneal was the reduction of the noise in the baseline resistance (R_0), as measured with the same datalogger. The ratio of noise to R_0 was reduced in all cases, ranging from a factor of 2 to as much as 27x.

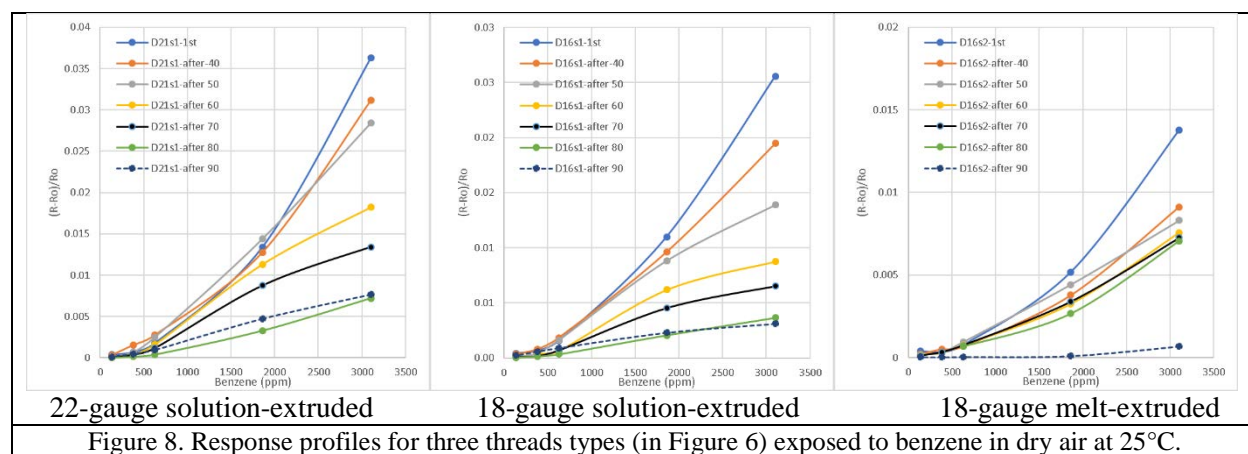
During the first anneal, as the pristine threads were heated to 40°C, the resistance in air increases gradually with increasing temperature (Figure 7); however, when threads are held at a constant temperature of 40°C, in all cases, resistances of the threads gradually drift to lower values.



We note also that the melt-extruded thread (Figure 6d), while having a relatively low resistance, is not fully annealed, as it still underwent significant changes during successive anneals. This suggests that the structure was locked-in as the thread was quenched during its extrusion from the 150°C syringe. We observe that its temperature sensitivity during the first 40°C anneal is similar to the solution extruded threads in the figure above.

The direction that the resistance changes with temperature flips, from a positive temperature relation to negative, after the 80°C treatment for all of these threads. During the first heating of these 18- and 22-gauge solution-extruded threads, from 25°C to 40°C, the average temperature coefficient of resistance (TCR) was 0.003683 Ω/Ω/°C ± 0.000604 Ω/Ω/°C, with the melt-extruded thread being the highest at 0.005619 Ω/Ω/°C. After the 90°C anneal, the average TCR (measured from 20°C to 40°C) was -0.000569 Ω/Ω/°C ± 0.000035 Ω/Ω/°C for the solution-extruded threads, and -0.0001595 for the melt-extruded thread. We believe that the denser structure of the melt-extruded thread makes it less temperature sensitive in its final state.

Figure 8 shows the response characteristics for three extruded threads as pristine devices and after each of the thermal treatments.



After each successive treatment, the responses ($\Delta R/R_0$) decrease until the 80°C for the solution-extruded threads. The melt-extruded thread appears to have a significant decrease after 90°C.

In terms of limits of detection, however, we observe that the noise improves as the sensors are annealed, with the most notable changes occur after the 70°C anneal. Where the LODs (Figure 9) decrease (improve) and continue to improve with higher thermal treatments. Both the LOD and the exposure to exposure consistency (error bars) improved after the high temperature anneals.

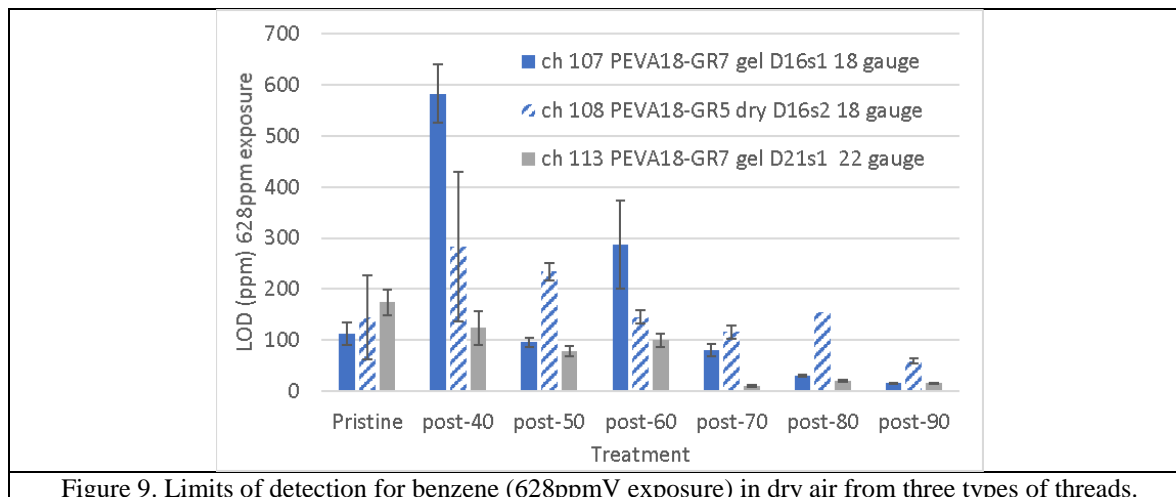
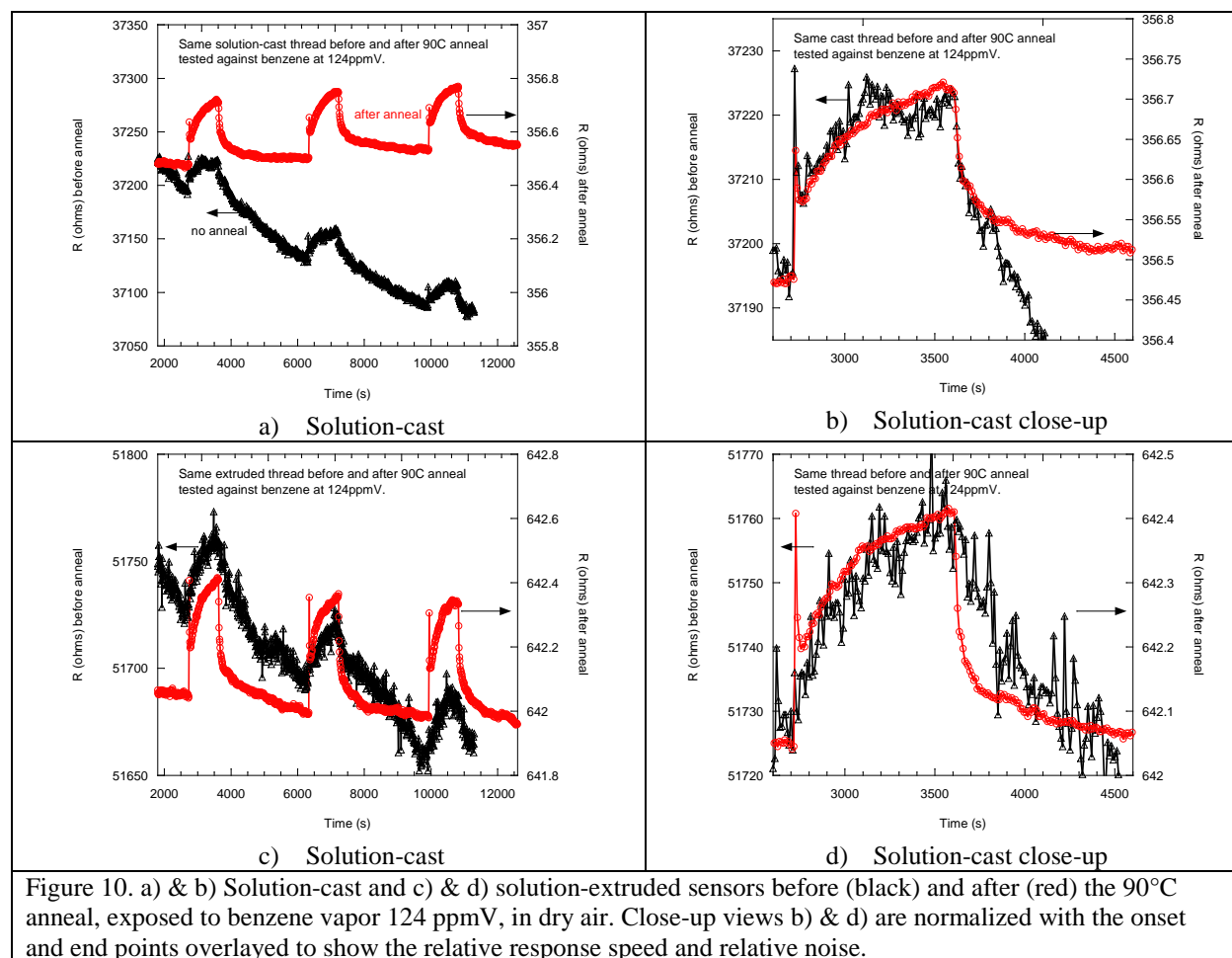


Figure 9. Limits of detection for benzene (628ppmV exposure) in dry air from three types of threads.

These observations are consistent when new pristine samples were heated directly to 60°C, retested, and then heated to 90°C and retested. Similarly, if the pristine samples are heated directly to 90°C, the results are similar, suggesting that final treatment is of sufficient duration, as to set the final state, so the incremental treatments do not have permanent effects.

For comparison, solution-cast segments of slices were evaluated in parallel to the solution-extruded threads, and we observe that the behavior of these (thicker and denser) films is consistent with the threads, with the exception that the different in starting and ending resistances being lower for the cast samples. Both types of samples were exposed to benzene vapors after each thermal treatment to compare sensitivity. Figure 10 shows the raw responses from pristine (left axes) and 90°C-annealed samples (right axes).

The standard error ($SE = \text{stdev}/\text{avg}$) of the baseline is 5.4×10^{-5} (pre anneal), and 6.7×10^{-6} post anneal. For a ceramic 50kohm and 5kOhm resistor in the same test setup, the SE was 6×10^{-6} and 2×10^{-6} , respectively. This suggests that the sensor is more noisy pre-anneal, rather than the noise being an artifact of the measurement setup.

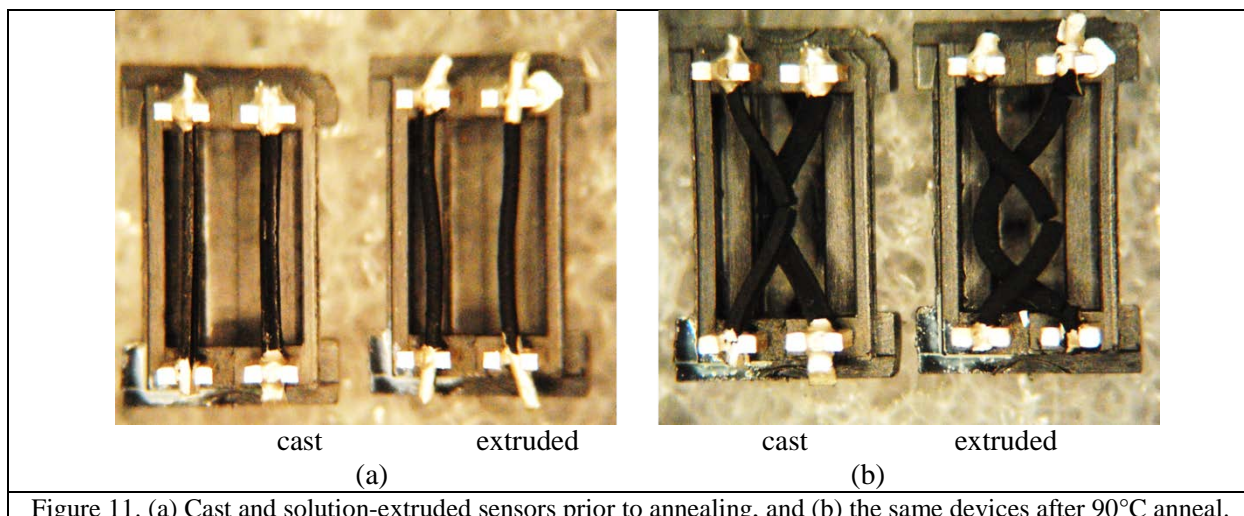


After the 90°C anneal, the starting resistances are significantly lower, and the size of the resistance change upon vapor exposure is also reduced. We also note that the drift is reduced, and the speed of response is increased after annealing, which is most obvious as the benzene vapor is removed from the system and the sensors recover to baseline. Before annealing at 90°C the average response ($\Delta R/R_0$) to 124 ppmV of benzene was 0.0005 ± 0.00004 and 0.00059 ± 0.00006 vs. 0.00061 ± 0.00006 and 0.00064 ± 0.00003 for the extruded and cast samples, respectively. This resulted in an improved limit of detection by factors of ~12 and 3 for the extruded and cast samples, respectively (Table 6).

Table 6. Limits of detection improvement due to 90°C anneal on solution-cast and -extruded samples.

Type	LOD (ppm) Pristine	LOD (ppm) Post-90°C anneal
Solution-extruded (18-gauge)	48 ± 9	3.9 ± 0.6
Solution-cast	21 ± 9	6.6 ± 2.9

The inner diameter of an 18-gauge needle is 0.84mm. When dried, the solution-extruded threads are on average 0.46mm in diameter, i.e. there is significant volume reduction as the toluene evaporated from the threads. We must note that the higher temperature anneals make the threads more fragile, as the annealing at 90°C had a significant effect on their shape (Figure 11) causing visible volume expansion, and, in some cases, resulted in cracks or breaks if both ends were held rigidly.



Note the increase in thickness and length of both the solution-cast and solution-extruded devices (Table 7). When heated to 90°C and unconstrained by the package, the solution-extruded threads bend, as the stress is apparently not consistent on all sides. The solution-cast segments, which are thicker, stay straighter when unconstrained.

Table 7. Average percentage volume expansion of (90°C) annealed samples (2 of each type.

Measured Dimension	Solution-cast	Solution-extruded
Length	4.0%	18.3%
Average thickness	5.4%	
Average Width or Diameter	10.8%	14.8%
Volume	27%	69%

When heated to 50°C or more, during the anneals, we observe a characteristic maximum in the resistance, that occurs at 42.5°C ± 2.2°C and 45.7°C ± 3.6°C for the solution extruded and cast devices, respectively (Figure 12).

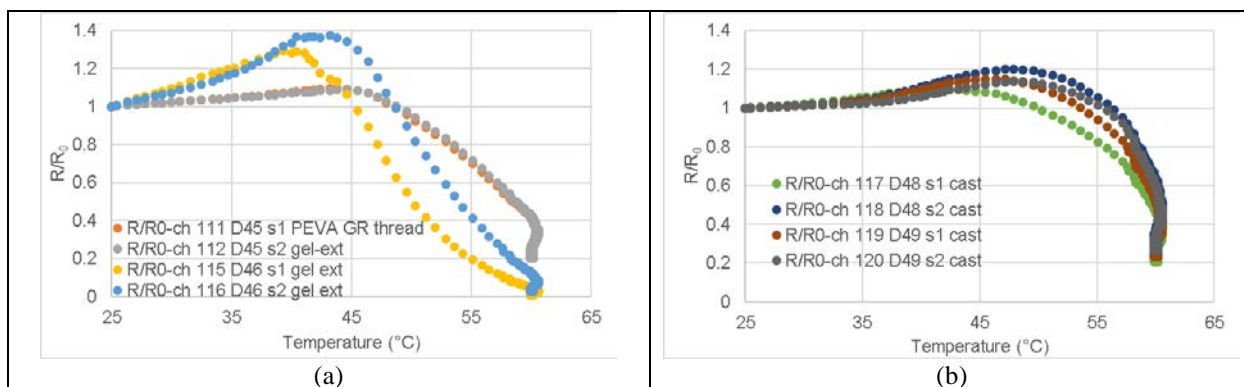


Figure 12. Pristine (a) solution-extruded (b) solution-cast samples during first heating to 60°C. Heating rate was 9.5°C/min.

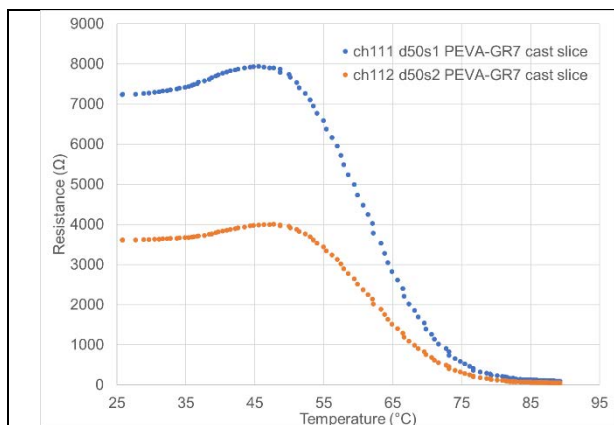


Figure 13. Pristine solution-cast samples first heating to 90°C. Heating rate was 7.5°C/min.

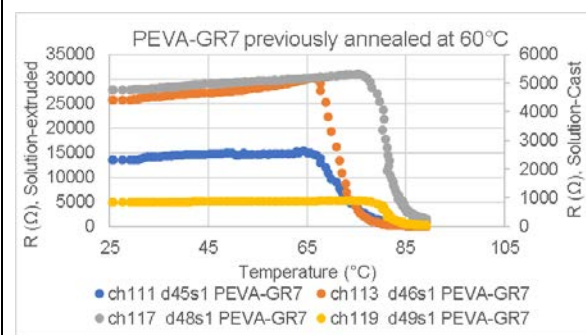


Figure 14. Previously 60°C-annealed solution-extruded and cast samples, first heating to 90°C

In the sample heated directly to 90°C (Figure 13), the maxima occur at 46.6°C ± 1.5 (cast), which is in-line with the devices heated only to 60°C. Further heating of these devices to 90°C (Figure 14), causes a second resistance maximum at 65.5°C ± 1.1°C and 73.4°C ± 2.2°C, for the solution extruded and cast devices, respectively.

With the solution-cast samples, annealing to 120°C and 129°C (Figure 15, Figure 16) yielded some improvement in the device sensitivity (Figure 17 and Table 8), however the extruded threads became too fragile and were not usable after these treatments. The cast segments were also more brittle after the high temperature treatments, but were thick enough to still be attached to the support pins for measurement.

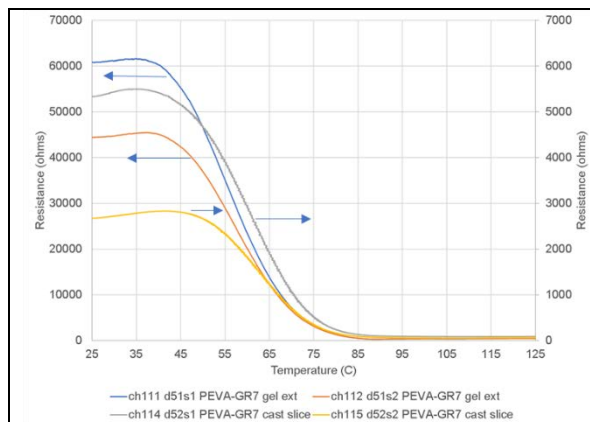


Figure 15. Resistance traces for pristine solution-cast and solution-extruded samples heated to 129°C.

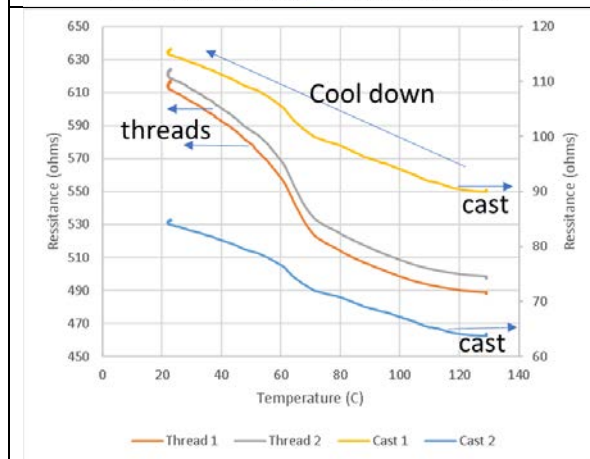


Figure 16. Resistance of solution-cast and solution-extruded samples tracked during cool down from 129°C. Upon cooling from 129°C, both the solution-cast and solution-extruded samples (2 each) show a resistance shift occurs between 60°-75°C that is characteristic of the PEVA freezing point (64°C Dupont Elvax 460).

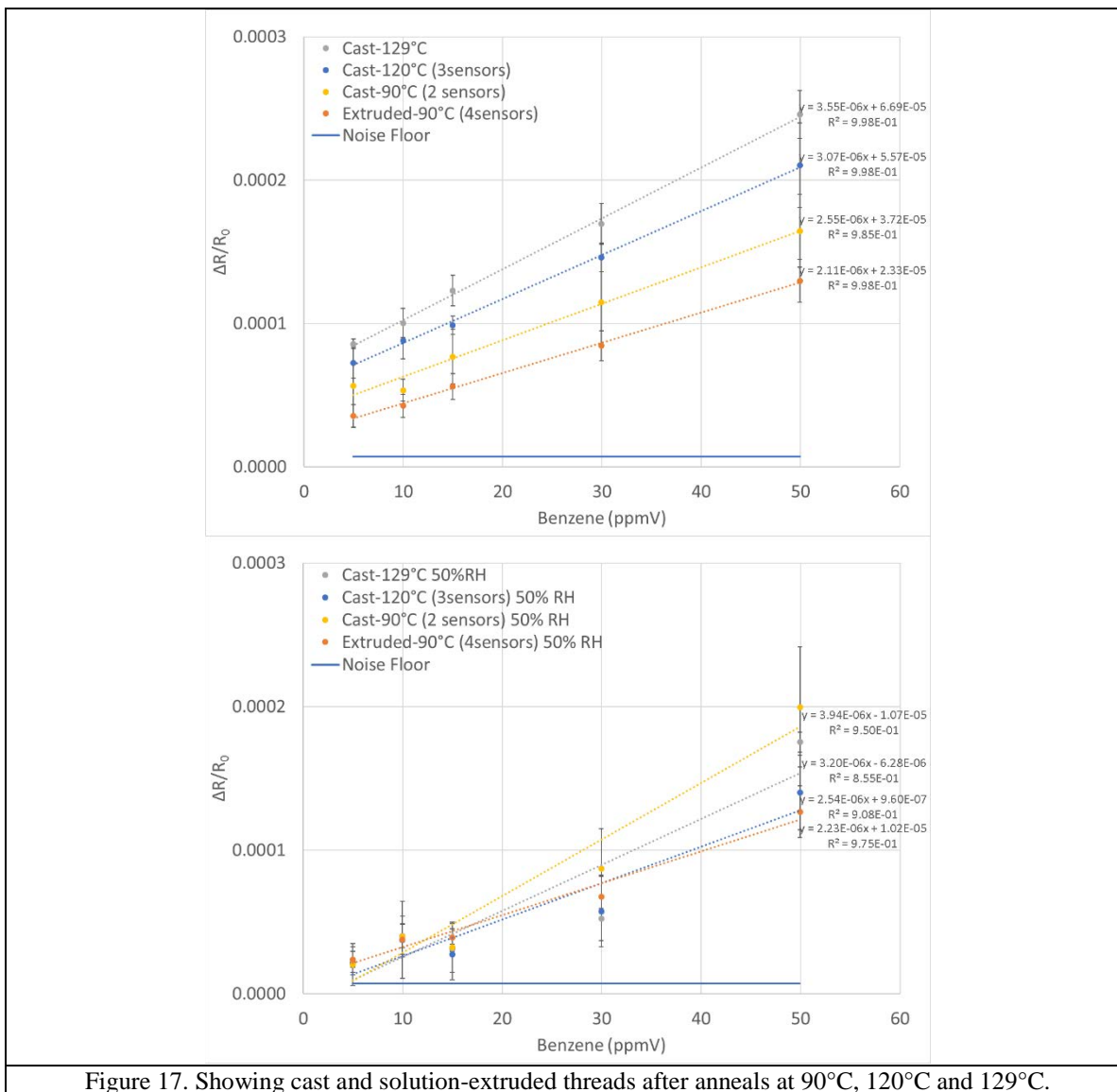


Table 8. Limits of detection for benzene from Figure 17 data in dry air and 50% humidity at 25°C.

Condition	Cast-129°C	Cast 120°C	Cast 90°C	Extruded 90°C
Dry Air	1.5 ± 0.1	2.2 ± 0.4	2.5 ± 2.1	2.4 ± 0.6
50% Humidity	8 ± 1	8 ± 4	9 ± 6	4 ± 3

The measurement noise (averaged of 10 sensors used in Table 8 calculations) in dry air and humid air from these tests was nearly identical, $7.0 \times 10^{-6} \Omega/\Omega$ vs. $7.3 \times 10^{-6} \Omega/\Omega$, respectively. Some longer-term (minutes) variability can be attributed to the humidity control, which can add to the observed error in the responses. The presence of humidity also diminishes the response, as the large amount of water vapor competes with benzene for binding sites in the polymer. Even though, PEVA does not have a significant sensitivity to humidity, the acetate group in the polymer is available for hydrogen-bonding with the water. This may act to reduce the swelling of the polymer when benzene is added.

Adjacent samples from the solution-cast material was submitted for differential scanning calorimetry (DSC). DSC endotherms from pristine, 60°C annealed, and 90°C annealed solution-cast samples. DSC was performed with a ramp (10°C/min) from 25°C to 550°C (Figure 18).

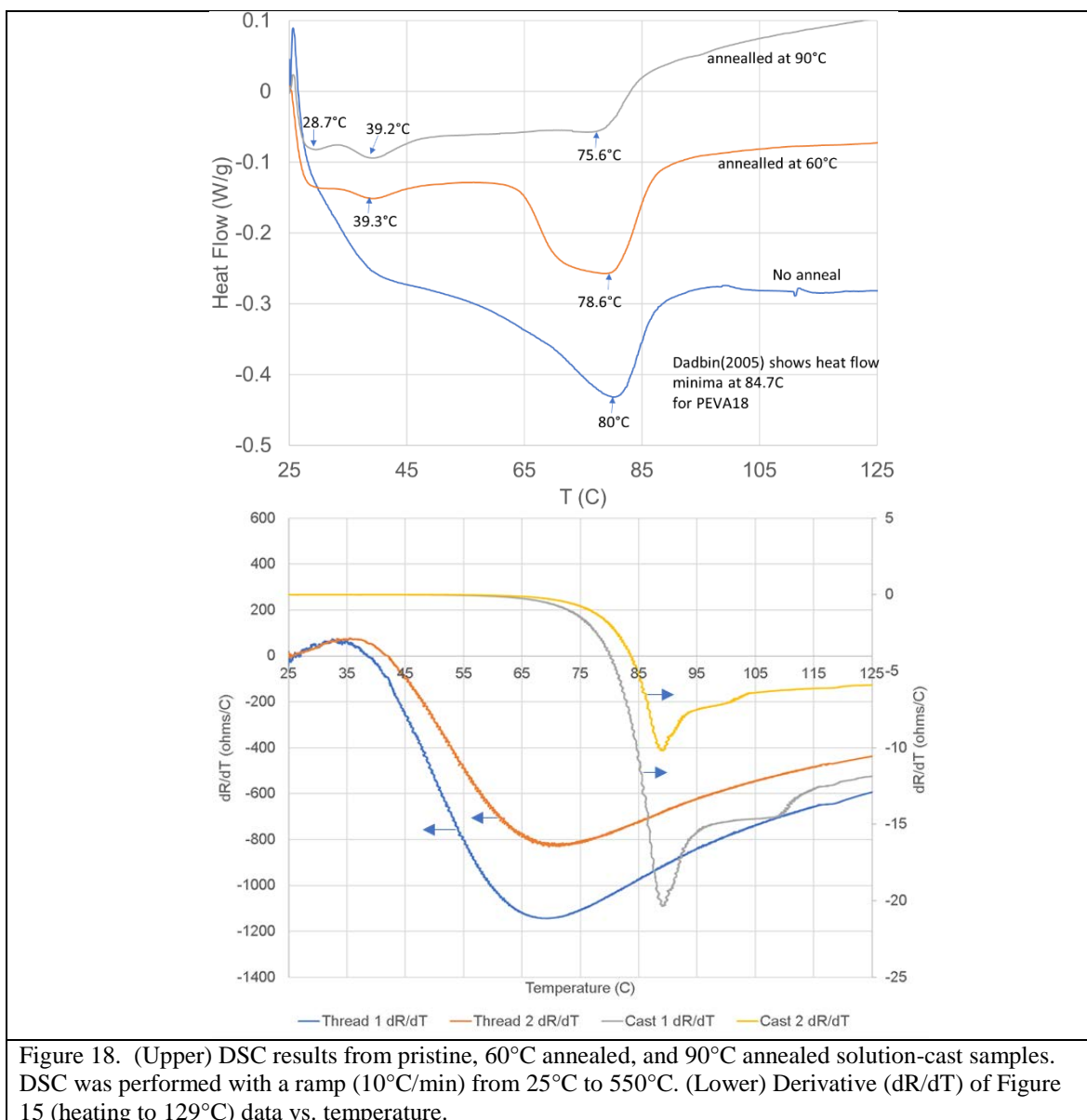


Figure 18. (Upper) DSC results from pristine, 60°C annealed, and 90°C annealed solution-cast samples. DSC was performed with a ramp (10°C/min) from 25°C to 550°C. (Lower) Derivative (dR/dT) of Figure 15 (heating to 129°C) data vs. temperature.

Two observations are clear from these results: first, that the points of inflection that coincide with vinyl acetate (49°C) and polyethylene (77°C) melting are much smaller in the annealed samples than the pristine sample³³; second, the resistances for cast samples heated to 129°C show a more distinct transition near the specified melting point (88°C) of PEVA18%, which is similar to the reported bulk melting point (85.6°C, Dadbin³⁴, 88°C, Dupont³⁵, 87°C, Sigma Aldrich data sheet) of undoped PEVA18.

In contrast, the solution-extruded threads, show a broad decrease in resistance (valley), which may indicate a broad range of crystal sizes in these samples. We attribute this to the different fabrication methods, since the cast material was allowed time to settle and recrystallize as the solvent evaporated from the large sheet. The sheet is likely to have reduced its thickness as it dried, more than its width. The extrusions were thin, cylindrical shapes, having much smaller diameter, which could dry faster, leaving less time to rearrange and recrystallize at different rates as the toluene diffused out from the center. The thread likely shrank radially more quickly and uniformly, reducing its total diameter.

In the DSC results, we observed that the transitions coincide with the observed maxima in the resistance measurements above. The area of the valley is indicative of the degree of crystallinity of these

polymers, and the noticeably reduced areas with successive anneals indicates that the PEVA-GR7 annealed at 90°C has reduced crystallinity, compared to the pristine and 60°C annealed sample. Also, we observe that the melting point is gradually shifted lower with higher temperature anneals.

We speculate that the presence of graphene is intercalating into melted crystals, and inhibiting PE crystal growth as the annealed samples are cooled, thus locking in a more amorphous structure. The less crystalline PEVA and better distributed graphene then allow for improved conductivity, lowering the baseline resistance. The associated increased surface area improves speed of response during vapor exposure. This is consistent with the observations of Heuchel³⁶, who observed the disappearance of the first valley between 30°C and 50°C, during a second heating, of an un-doped, non-crosslinked PEVA18 (Elvax 460) sample. They suggest that the reduced valley is due to reduced crystal size, as a result of the previous heating.

Samples were investigated using scanning electron microscopy (SEM) to study the morphology of the polymer-composite. Both solution-cast and solution-extruded samples were studied, in as-fabricated and 90°C annealed forms. In Figure 19, the unannealed, solution-cast sample surface is smoother than the extruded sample (Figure 20), with regions of varied surface texture, ranging from smooth or amorphous to mottled with bubbles (>1µm to ≈ 50nm). The cross-section of the solution-cast sample appears relatively more uniform in texture. The figures show close-ups view of three distinct surface textures (Figure 19 c, d, e).

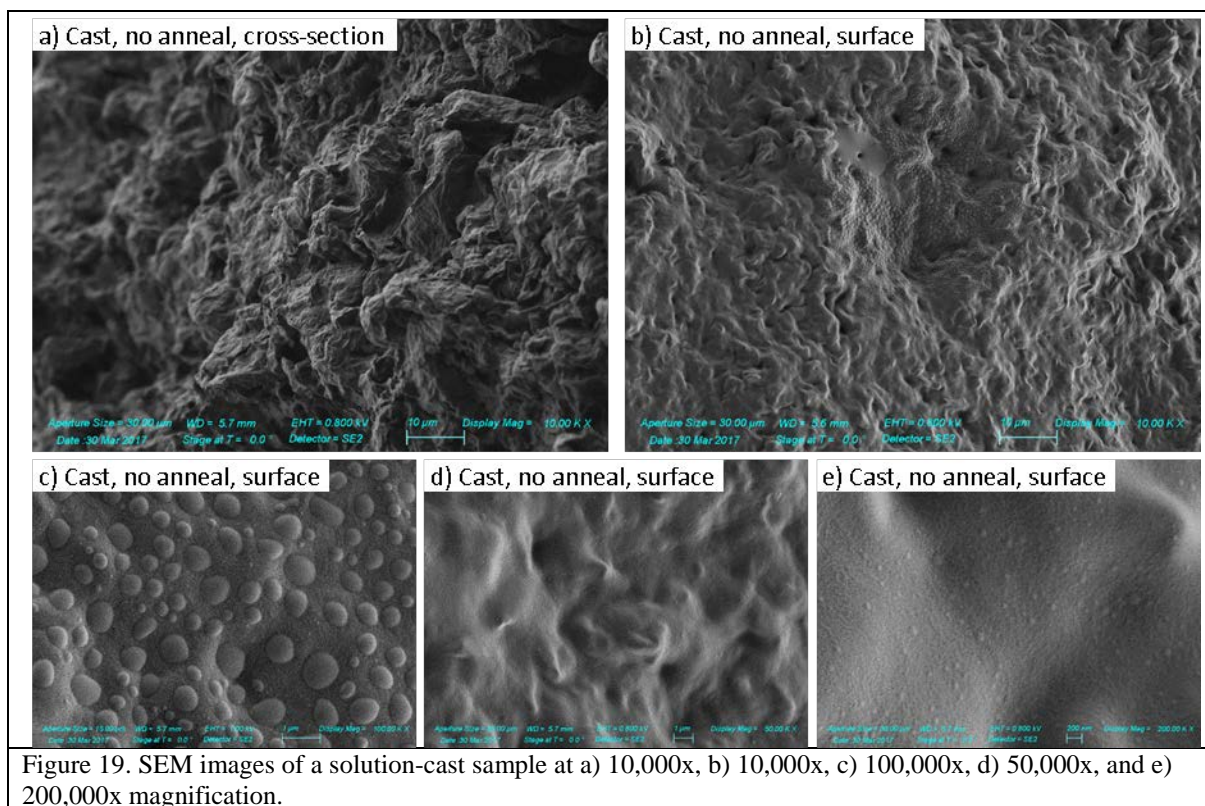


Figure 19. SEM images of a solution-cast sample at a) 10,000x, b) 10,000x, c) 100,000x, d) 50,000x, and e) 200,000x magnification.

In contrast to the solution-cast sample, the solution-extruded surface morphology is more jagged, with regions of sharp features (few µm to 10's of µm) in a background of more amorphous material. This is likely due to the shearing and stretching of the bubbles (air or solvent) that occurred when the sample was forced out of the steel syringe needle. The bottom row of the figure shows close-up views of a jagged feature and the smooth amorphous area surrounding it. It is unclear from this work if the sharp features are graphene nanoplatelets (7% by weight, 3% by volume) or, more likely, crystalline regions of the polymer (25%, Heuchel³⁶, 2015 and 26%, Hiss³⁷, 1999).

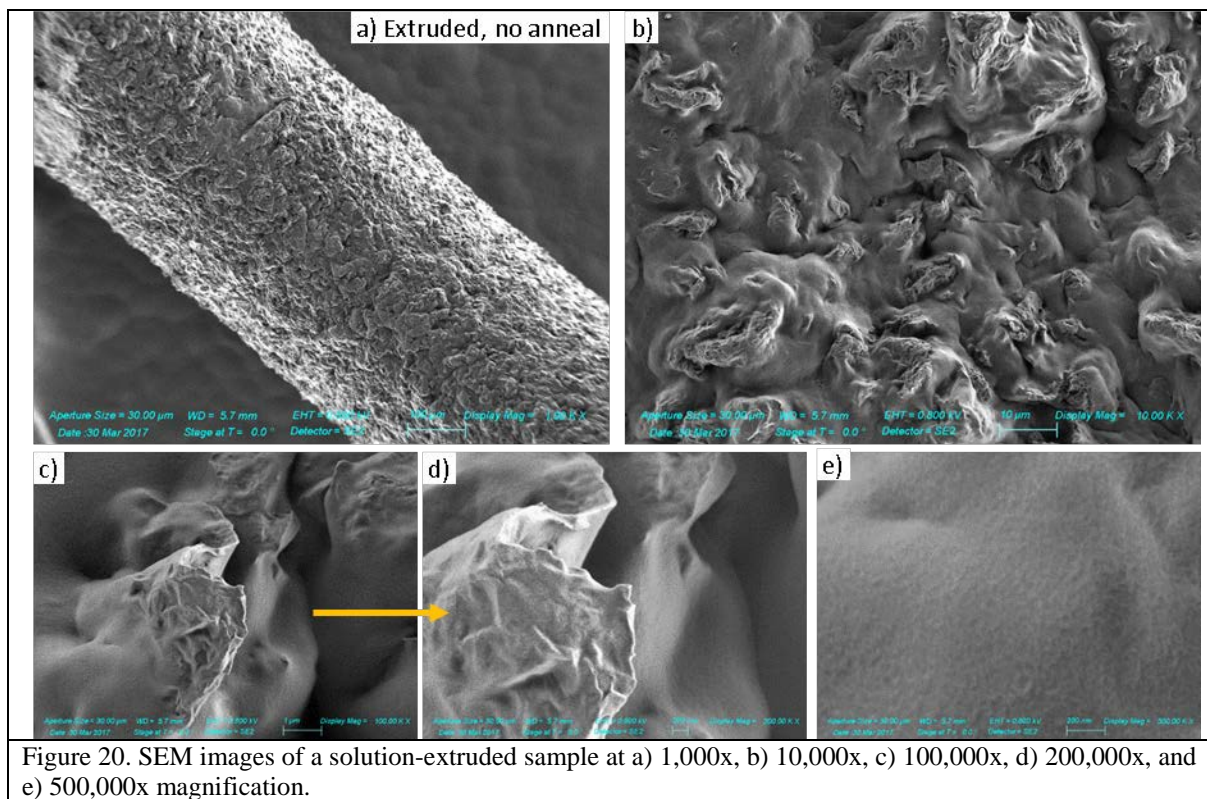


Figure 20. SEM images of a solution-extruded sample at a) 1,000x, b) 10,000x, c) 100,000x, d) 200,000x, and e) 500,000x magnification.

The result of the 90°C anneal is a significantly rougher surface texture on the cast sample (Figure 21) and the extruded sample (Figure 22), and the two sample types are now less distinguishable.

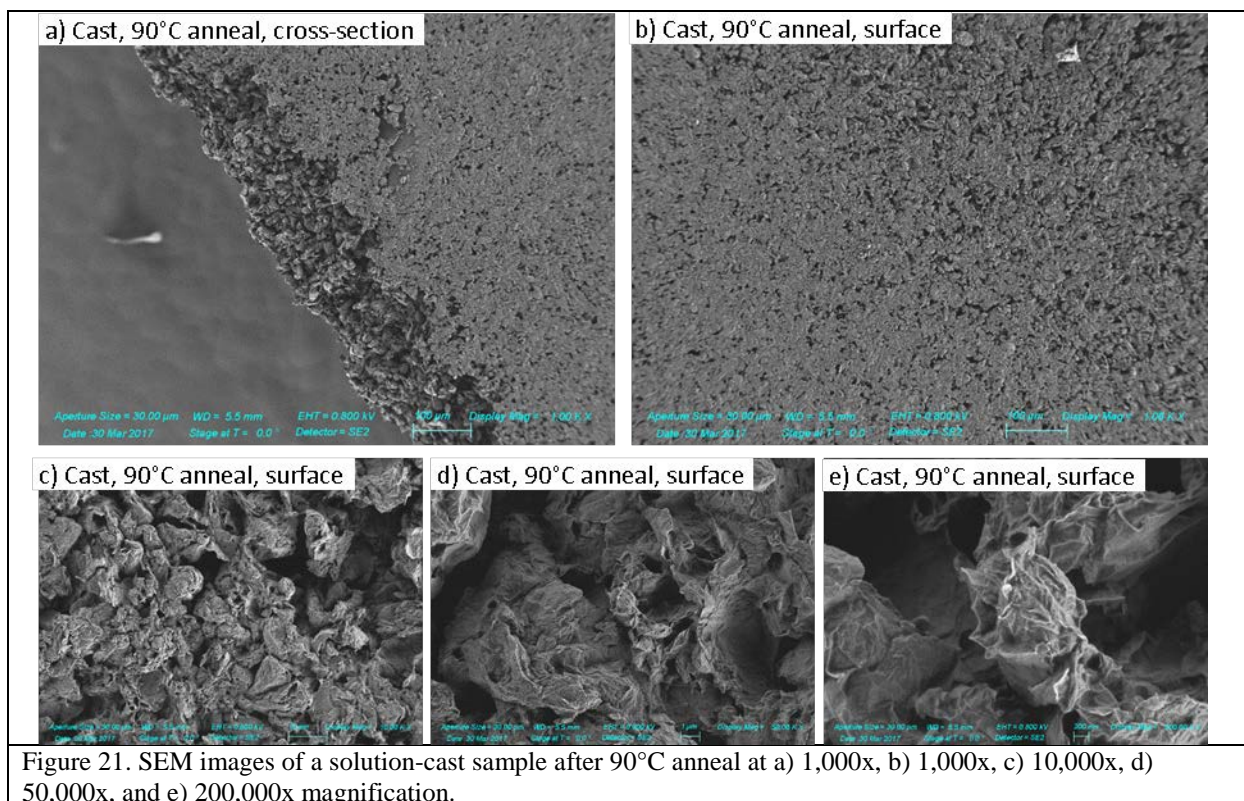
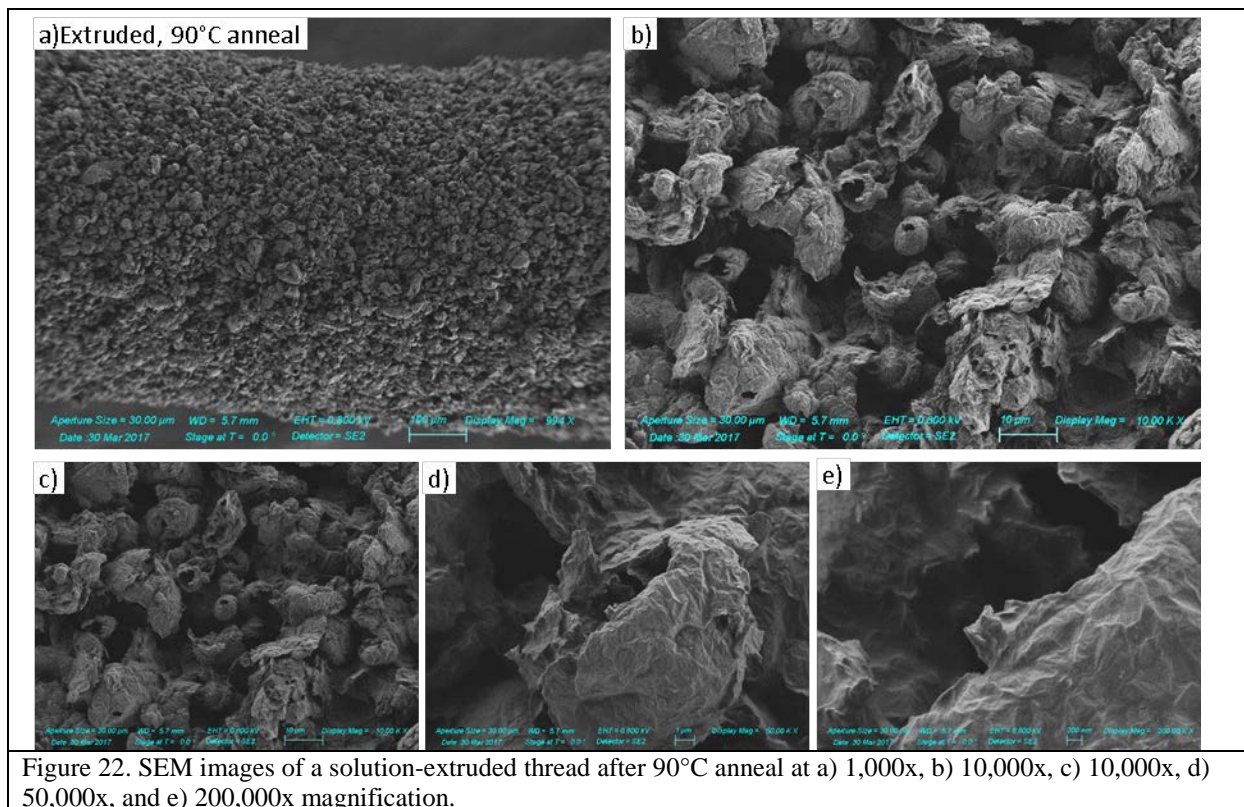


Figure 21. SEM images of a solution-cast sample after 90°C anneal at a) 1,000x, b) 1,000x, c) 10,000x, d) 50,000x, and e) 200,000x magnification.



On a large scale, the surface morphology has become more consistent in appearance across the entire sample, with rugged terrain, and the polymer forming thin-walls ($\ll 1\mu\text{m}$) around voids or pores where the open holes have the appearance of torn edges. The volume expansion of the extruded thread is obvious when compared to the unannealed sample at the same magnification. Note that the extruded sample still retained its cylindrical shape.

Both types of samples, cast and extruded, expanded after the anneals (Table 7). The annealed samples have significantly reduced baseline resistances (in dry air), reduced noise, shorter response times, and improved limits of detection (LOD) for benzene.

The faster responses may be attributed to the increased surface area and reduced density allowing for faster vapor sorption.

However, the baseline (dry air, 25°C) resistances of both types of annealed samples are significantly reduced (dropping from tens of $\text{k}\Omega$ to $<500\Omega$), which is counterintuitive to the reduced density. This suggests that the lower, post-anneal resistances are a result of the reduced crystallinity of the polymer, which is confirmed by DSC (Figure 18). In addition, the less-crystalline state may also allow the graphene to distribute more uniformly through the bulk as the polymer melts and rearranges.

Specific Aim 2) Demonstrate low-cost volume manufacturing path using commercial micro-extrusion.

Milestone 2: Working with Randcastle to fabricate thread samples using micro-extruder. Determine which materials can be extruded and how to incorporate graphene into the composites.	Task modified
Metrics:	
(a) array of threads fabricated	√
(b) preliminary recipes established.	√

Task 2) Fabricate threads using commercial micro-extruder:

For this task, Seacoast deviated from the original work plan. Originally, we had planned to take raw materials to a contract lab (Randcastle, Inc., New Jersey) where we could use a commercial micro-extruder to demonstrate melt-extrusion fabrication of the chemiresistive threads. The research strategy was originally submitted in Feb. 2015, but not funded until Sept. 2016. In the interim, we determined that the method of melt-extrusion as proposed, using a commercial micro-extruder was unlikely to be successful, mainly due to two reasons: 1) the polymer properties achieved with melt extrusion produced sensor that were not useful for chemical sensing, and 2) the relatively small number of recipes we could evaluate, the large quantity of starting material needed for these machines, and the time involved.

Common extruders use a significantly large amount (kilograms) of polymer, however, the Randcastle micro-extruder system we investigated allow the use of ~50 grams of material, allowing for losses. Still this was 100 times the amount needed for Phase I test purposes. In addition, the cost of enough graphene for such testing combined with the labor cost to compare a sufficient number of recipes to obtain statistically meaningful data was beyond the available budget.

Given the available resources, we compared the melt properties of various polymers known to be sensitive to benzene and the other fuel-related chemical targets. We constructed a custom heated-syringe extrusion instrument using a Teflon plug moving inside a barrel that could be pushed to extrude the nanocomposite material through a narrow-gauge, stainless steel syringe tip. Our instrument has almost no dead volume, thereby providing maximum efficiency in materials usage. The heated system simulates the extruder portion of the commercial micro-extruder without the large dead volume and mixing stages. The resulting threads following melt-extrusion at 150°C, however, proved substantially insensitive as sensors. The threads were notably denser, as a result of being formed without solvent, and the high density, inversely correlated to surface area needed for absorption of chemical vapor, resulted in extremely slow and relatively small sensor responses.

Therefore, the majority of Task 1 (above) focused on solution-cast and solution-extruded samples, which were more successful, and still compatible with high-volume, low-cost manufacturing that will be needed to fabricate such sensors in large volume. Table 9 compares the strengths and weaknesses of the three manufacturing techniques for producing chemical sensing threads, based on our Phase I work.

Table 9. Strengths and weaknesses of the various thread fabrication methods.

	Melt-extrusion	Solution-Extrusion	Solution-Casting
Advantages	<ul style="list-style-type: none"> • Commonly used for clothing fibers • Die or syringe needle can be used to control thickness 	<ul style="list-style-type: none"> • Does not thermally set the polymer, • Provide less dense, more porous fibers, • Die or syringe needle can be used to control thickness 	<ul style="list-style-type: none"> • Lowest cost method, • Can use molds to form threads of different dimensions
Disadvantages	<ul style="list-style-type: none"> • Formed denser threads that were slow to respond 	<ul style="list-style-type: none"> • Requires a solvent, that must be removed from the product, • Potential worker exposure to noxious solvent vapors during fabrication of the threads, • More fragile than the melt-extruded threads 	<ul style="list-style-type: none"> • Requires a solvent, that must be evaporated • Thickness control may be an issue, unless a mold is used • Potential worker exposure to noxious solvent vapors during fabrication of the threads
Phase I performance	<ul style="list-style-type: none"> • Poor 	<ul style="list-style-type: none"> • Acceptable 	<ul style="list-style-type: none"> • Acceptable

As a result, we believe this fulfills the original intent of the task, which was to demonstrate viable chemical sensing threads fabricated using a low-cost manufacturable method. Based on the Phase I results (Task 1), we determined the solution extrusion and solution-casting methods are acceptable to continue with further development and optimization. We are confident that improvements in the limits of detection for Benzene can be made with more focus on optimizing the chemiresistor formulations.

Specific Aim 3) Determine effects of environmental and physical variables on the threads/arrays.

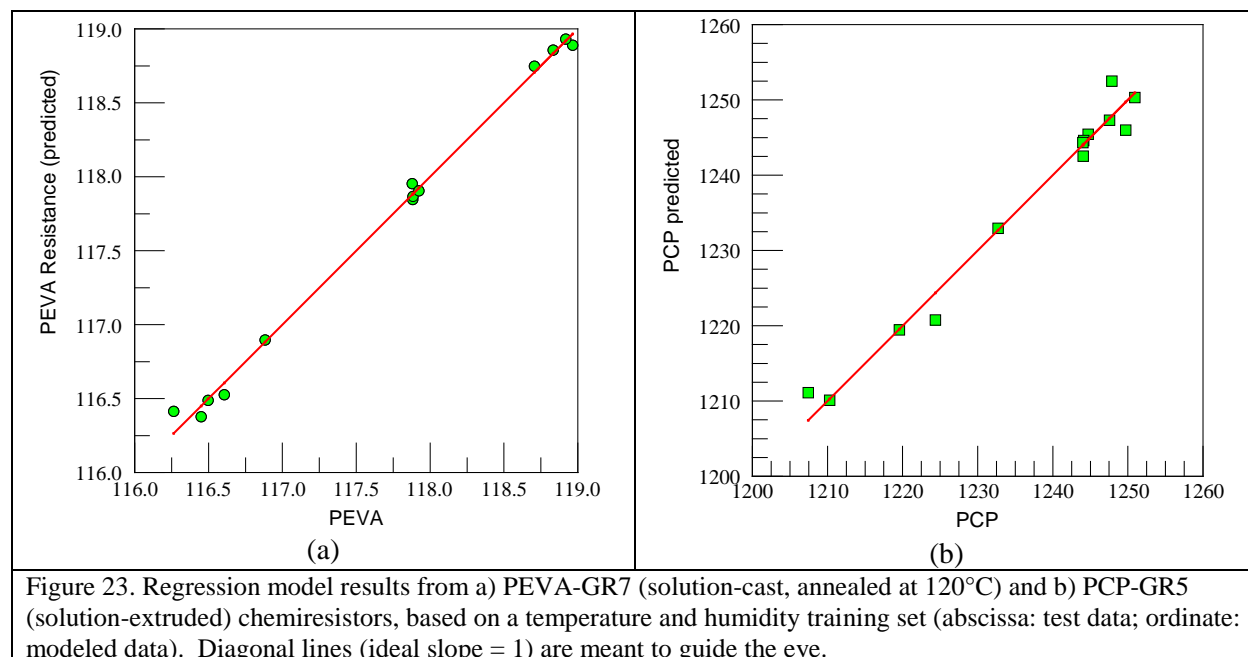
Milestone 3: Threads and electronics tested against electrostatic discharge (ESD), bending, temperature, humidity to determine the effect of these variables, and need for compensation and physical or electrical protection of the device.	√
Metrics:	
(a) Algorithms developed for compensating for temperature and humidity;	√
(b) Designs developed for compensating for ESD and bending.	√

Task 3) Investigate effects of mechanical and environmental stressors:

Temperature and Humidity: From vapor testing with high humidity and varying temperatures (Task 1), we concluded that a humidity and temperature compensation is necessary to accurately estimate vapor exposures. Data was generated at 3 temperatures (10, 25, 40°C) and 4 humidity levels (0%, 25%, 50%, 70%). Using this training data from the chemiresistors, a multiple linear regression model was setup to take into account the expected environmental field variations in temperature and humidity. The goal is to accurately model R_0 at any condition where no chemical is present (within the limits tested). Figure 23 shows the results of the regression of the training data from the four chemiresistors in the form of:

$$R_{\text{sensor}(j)} = a_j T + b_j T^2 + c_j / T + d_j / T^2 + e_j RH + f_j RH^2 + g_j / RH + h_j RH^2 + i_j, \quad (1)$$

where the measured humidity and temperature were the independent variables (RH and T) and the measured resistances were the dependent variables (R); a to i are constants that the modeling software determines and j represent each sensor (polymer) in the array.



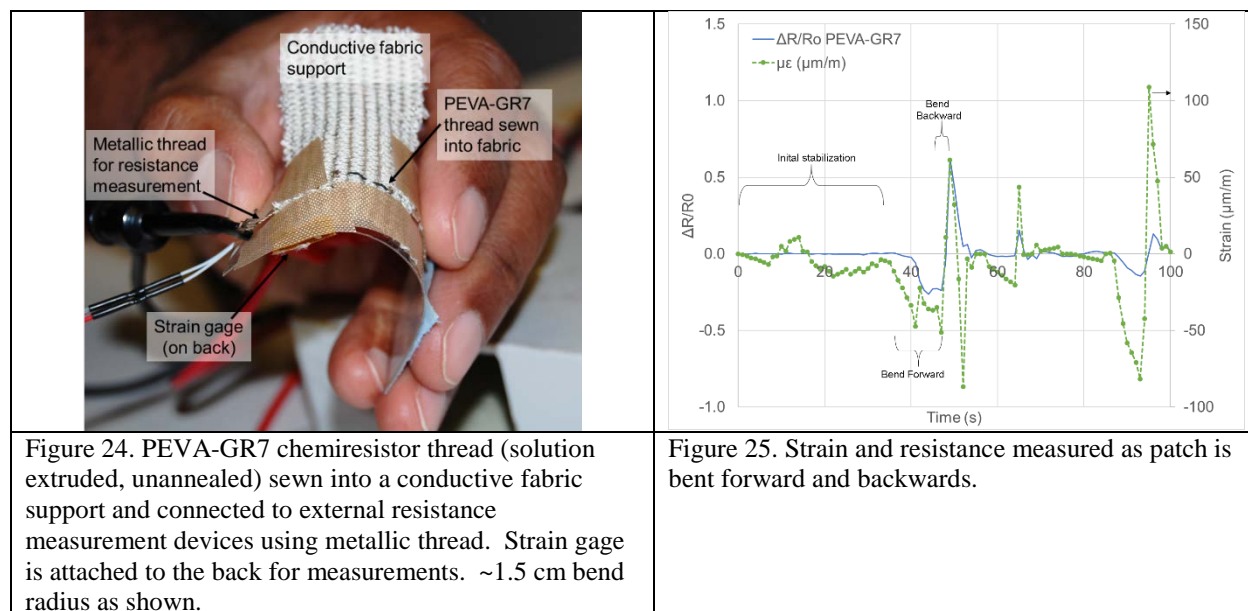
The regression terms were selected from previous work where the behavior of a number of sensors was modeled with respect to chemical concentrations.³⁸ The linear and nonlinear terms are based on observations of the raw data. One notes here that some sensors are better modeled than others. PEVA's low humidity sensitivity makes it easier to model versus PCP, which has a mildly higher humidity sensitivity. In the plots, deviations from the diagonal are representative of the error from ideal.

Bending Strain: Although somewhat fragile, PEVA-GR7 threads were capable of being sewn into a commercial-off-the-shelf conductive fabric, using a common sewing needle, confirming our original goals of developing these materials into sewn patches. The conductive fabric is made from a fabric mesh, with metal wires sewn in parallel lines, spaced about 1mm apart. This assembly mimics a common, electronics prototyping circuit board, and is ideal for evaluating the developed materials.

A commercial strain gage (Omega #KFH-10-120-C1-11L1M2R, 120Ω, gage factor, GF= 2.07 ±1%) was attached to a thin plastic support, which was taped to the back of the patch (Figure 24). This allows transfer of the strain to the gage without the adhesive of the gage causing a change in the thread's physical attachment to the fabric. At constant temperature, the strain ($\Delta L/L$), ϵ , is calculated from the resistance change (ΔR) in the gage, which was measured using a Wheatstone bridge (Equation 2).

$$\epsilon = \Delta R/R_0 / GF \quad (2)$$

where R_0 is the unstrained resistance. Figure 25 shows the measured strain and resistance of a PEVA-GR7 thread as the patch is bent forward and backward.



The resistive threads were significantly sensitive to bending. The maximum bend (minimum radius) tested was approximately 1.5cm (both concave and convex), but even with much shallower flexing, the resistance changes much more than a typical chemical sensor response to 100ppm of benzene. We believe the points of contact between the polymer-thread and the metallic thread used for electrical connectivity were the most sensitive and likely points of failure. Electrical and algorithmic compensation alone are unlikely to be successful in distinguishing mechanical responses from chemical responses due to the errors generated by the high strain-sensitivity. However, inclusion of an appropriate reference device to compensate for mechanical strains is envisioned to deal with this issue. Thus, from strain gauge tests, we

conclude that a supportive backing may be needed to keep threads rigid, primarily due to the strain applied to the electrical contacts with the threads.

ESD: ESD compensation from motion or physical contact was determined to be a non-factor, after we determined that the threads required a semi-rigid support and that a membrane would be placed over the sensors to protect them from physical abrasion and from liquid contact. Figure 26 shows one of Seacoast's current MEMS-based chemical sensors with a GORE-TEX vent preventing the water droplet seen in the photo from reaching the sensor below. These membrane vents are available in a variety of shapes and sizes and are commonly used in sensor applications, and can be teamed with metal mesh supports if grounding is needed for protection from electrical interference.

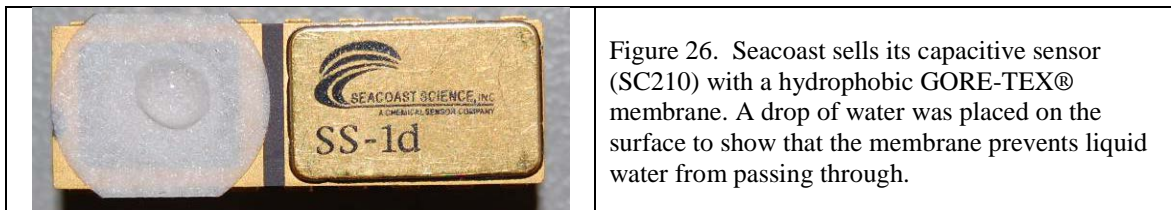


Figure 26. Seacoast sells its capacitive sensor (SC210) with a hydrophobic GORE-TEX® membrane. A drop of water was placed on the surface to show that the membrane prevents liquid water from passing through.

2.5 Conclusion and Summary

Phase I of this NIOSH SBIR project focused on demonstrating petrochemical fuel detection with chemically sensitive polymer-nanocomposite threads that could be included in smart-fabric apparel and personal protective gear. The target application for the sensing threads is for low-cost integration into wearable patches that can act as personal exposure monitors, when teamed with measurement and logging electronics.

All objectives of the Phase I proposal have been achieved and the study clearly showed the feasibility of the proposed concept of fabricating chemical detection threads sewn into conductive fabric templates and detecting chemicals in the air, particularly for personnel working around petrochemical fuels. Ultimately, the threads can be made into the proposed chemical sensing patches. The Phase I work uncovered many challenges; however, Seacoast has demonstrated workable solutions to counter them.

The most successful threads were fabricated using either solution-casting or solution-extrusion of polymer-graphene composites, whose resistance increases substantially when exposed to the target chemical vapors, most notably benzene. Both fabrication methods are compatible with low-cost thread fabrication techniques; further development would be required to optimize either method for high-volume production of threads that are physically robust and chemically sensitive enough for the intended application.

The primary performance metric, limit of detection achieved from 15-min vapor exposures, was used to compare various formulations and fabrication methods. Based on these measurements, we achieved our primary goal of detecting below 10% of the NIOSH worker safety limits for toluene, isooctane, and isopentane. The selectivity of these threads varied by type of polymer matrix, while the sensitivity and speed of response were directly effected by physical characteristics of the threads and the thermal treatments they received during fabrication.

Benzene was the most difficult of the Phase I target analytes to detect at low concentrations. We spent significant effort in Phase I, developing fabrication techniques, and studying thermal treatments that could improve the sensitivity to benzene. Over the course of this study, we determined that the surface morphology could be enhanced to improve sensitivity by thermal treatment after initial forming into a thread. We also determined that the use of a commercial micro-extruder was incompatible with the process characteristics required of the sensors. This caused us to deviate from the original work plan (Specific Aim 2), to focus further on the solution-cast materials. Ultimately, we achieved a LOD of $1.5 \pm$

0.1 ppm for benzene, which is below the OSHA short-term regulation (5ppm), but not the NIOSH STEL (1ppm). We are confident that benzene sensitivity can be further improved by optimizing the graphene content of the nanocomposite formulation. Graphene content was generally held constant during this short concept demonstration to focus more effort on the polymer characteristics. We also believe the sensors can be made more sensitive by reducing the thread thickness.

We deviated from the original Phase I workplan by adding naphthalene as a Phase I target chemical, due to its abundance in jet fuels, the primary source of fuel vapor exposures for DOD personnel. In Phase I, we demonstrated sub ppm sensitivity to naphthalene (0.06 ± 0.01 ppm from a polycaprolactone-graphene nanocomposite), which is well below 10% of the NIOSH STEL and 8-hr TWA.

Because we found that melt-extrusion does not produce threads possessing the necessary chemical sensitivity, Specific Aim #2 (Demonstrate low-cost volume manufacturing path using commercial micro-extrusion.) and its related task was changed to focus on solution-cast and solution-extruded threads. Therefore, we did not require use of a commercial micro-extruder, which would have been a melt-extruder, and rather we were able to simulate a solution-extruder using common laboratory materials. Both solution-based methods to fabricate chemoselective threads were found to be compatible with low-cost fabrication, thus achieving successful completion of this goal.

In terms of physical or structural survivability, the most important concern discovered during strain tests (Specific Aim #3), is the need for improved electrical contact between the sensing element and supervisory electronics, and the need for physical rigidity to keep these contacts from moving. In Phase II, we propose to investigate further methods to securely attach the chemical sensing threads to electronics for data collection, processing and display or transmission.

Based on lessons learned in Phase I, we have developed a Phase II plan that would take advantage of the selectivity observed from the different polymers to develop exposure monitors for fuel-related compounds while rejecting responses from superfluous interferents. In Phase II, we will optimize the sensor threads using test results by: 1) expanding the range of environmental test conditions, 2) exploring polymer:graphene ratio to improve sensitivity to benzene and the other compounds, 3) developing algorithms to compensate for interferences and environmental conditions. As a second Aim we will investigate and develop an appropriate method to integrate the threads with a secure (electrically and physically) conductive cloth substrate and electronics.

Seacoast is currently developing a resistance read-out circuit that we expect will be completed by the time Phase II begins; therefore, we expect to focus Phase II on materials testing and system optimization, rather than developing new electronics. In Phase II we will build prototypes capable of logging and transmitting exposure concentrations. Prototypes will be tested in simulated real-world conditions, using mannequins, rather than human test subjects. Seacoast has a self-contained 29,000 cu ft. room, plumbed for vapor exposure testing, for the mannequin challenges, which will make testing faster and less costly than if human subjects are used.

Publications

None submitted to date.

Seacoast is currently preparing a manuscript describing the results of the SEM and thermal treatment work.

Cumulative Inclusion Enrollment Table:

Not Applicable

Inclusion of gender and minority study subjects

Not Applicable

Inclusion of Children.

Not Applicable

Materials available for other investigators

Not Applicable

Bibliography & References Cited

- ¹ S. V. Patel, M. W. Jenkins, R. C. Hughes, W. G. Yelton, A. J. Ricco, "Differentiation of Chemical Components in a Binary Solvent Vapor Mixture Using Carbon/Polymer Composite-Based Chemiresistors," *Analytical Chemistry*, 72 (2000) 1532-1542.
- ² R. C. Hughes, W. G. Yelton, K. B. Pfeifer, and S. V. Patel, "Characteristics and Mechanism of Ion-Conducting Polymer Films as Chemical Sensors," *Journal of the Electrochemical Society*, 148 (2001) H37-H44.
- ³ M.S. Freund, N.S. Lewis, "A Chemically Diverse Conducting Polymer-Based Electronic Nose," *Proc. Natl. Acad. Sci. U.S.A.* 1995, 92, 2652- 2656.
- ⁴ M. P. Eastman, R. C. Hughes, G. Yelton, A. J. Ricco, S. V. Patel, M. W. Jenkins, "Application of the Solubility Parameter Concept to the Design of Chemiresistor Arrays," *Journal of the Electrochemical Society*, 146 (1999) 3907-3913.
- ⁵ M. Benz, S. V. Patel, "Freestanding Chemiresistive Polymer Composite Ribbons as High-Flux Sensors," *J. Appl. Polym. Sci.*, 125(5) 2012, 3986-3995. doi: 10.1002/app.36538.
- ⁶ S.V. Patel, M. Benz, "High-Flux Chemical Sensors", Dec. 2, 2013, U.S. Patent Application 20140220703 #14/094,695, Patent Pending.
- ⁷ US Bureau of Labor statistics page on Mining: <http://stats.bls.gov/oco/cg/cgs004.htm>
- ⁸ U.S Energy Information Administration, SHORT-TERM ENERGY AND SUMMER FUELS OUTLOOK, Release Date: April 11, 2017, https://www.eia.gov/outlooks/steo/report/us_oil.cfm
- ⁹ U.S Energy Information Administration, Use of Energy in the United States Explained, https://www.eia.gov/Energyexplained/index.cfm?page=us_energy_use, accessed 5/2/17
- ¹⁰ Bureau of Labor Statistics, 2010 Census of Fatal Occupational Injuries, TABLE A-1. Fatal occupational injuries by industry and event or exposure, All United States, 2010, <http://www.bls.gov/iif/oshcfoi1.htm#2010>.
- ¹¹ Bureau of Labor Statistics, News Release, USDL-11-1612, Table 16. <http://www.bls.gov/iif/oshcfoi1.htm#other>
- ¹² Bureau of Labor Statistics, News Release, USDL-11-1502, Table 6b. <http://www.bls.gov/iif/oshcfoi1.htm#other>
- ¹³ <http://www.buydraegertubes.com/petroleumhydrocarbons100a.aspx> (accessed 8/2/2014)
- ¹⁴ "Dräger-Tubes & CMS-Handbook 15th edition," Dräger Safety AG & Co. KGaA, Lübeck, 2008, pp. 232-233.
- ¹⁵ For example, the Dräger handbook page 114, specifications for denzene Dräger tubes states "Other aromatics (toluene, xylene, ethyl benzene) are indicated as well. It is impossible to measure benzene in the presence of these aromatics."
- ¹⁶ There are many distributors of single- and multi-gas detectors, these prices were taken from PK Safety: <http://www.pksafety.com/gasdetection.html>
- ¹⁷ There are no laws mandating calibration of portable gas monitors, as stated in the OSHA bulletin SHIB 09-30-2013 (<https://www.osha.gov/dts/shib/shib093013.html>). However, OSHA provides guidance based on ISEA recommendations that "A bump test . . . or calibration check of portable gas monitors should be conducted before each day's use in accordance with the manufacturer's instructions."
- ¹⁸ Agostino, P. N., R. J. LeBlanc Jr., and V. T. Jones III, 2002, Assessment of subsurface hydrocarbon contamination resulting from multiple releases at six former bulk-fuel storage and distribution terminals, Austin, Texas: A case study, in *Surface exploration case histories: Applications of geochemistry, magnetics, and remote sensing*, D. Schumacher and L. A. LeSchack, eds., AAPG Studies in Geology No. 48 and SEG Geophysical References Series No. 11, p. 299–325. Available at: <http://oberenvironmental.com/>
- ¹⁹ A list of organic compounds in fresh and weathered gasoline can be found at: <http://bcn.boulder.co.us/basin/waterworks/gasolinecomp.pdf>
- ²⁰ S. Uzaki, K. Adachi, T. Kotaka, "Multiple Dielectric Relaxations in Solid Polyorganophosphazenes," *Polymer Journal* (1988) 20, 221-229; doi:10.1295/polymj.20.221

- ²¹ S. T. Hobson, S. Cemalovic, O. Katzenelson, S. Steele, A. L. Thibadeaux, "Synthesis and QSPR of Polymers in Sensor Applications," Poster W113 presented at the Point Detection session, Chemical and Biological Defense Physical Science and Technology Conference, New Orleans, LA, 17-21 Nov. 2008.
[http://www.seacoastscience.com/Downloads/Hobson\(2008\)%20Polymer%20QSPR%20poster.pdf](http://www.seacoastscience.com/Downloads/Hobson(2008)%20Polymer%20QSPR%20poster.pdf)
- ²² D. Rivera, M.K. Alam, C.E. Davis, C.K. Ho, "Characterization of the ability of polymeric chemiresistor arrays to quantitate trichloroethylene using partial least squares (PLS): effects of experimental design, humidity, and temperature," *Sensors and Actuators B* 92 (2003) 110–120
- ²³ A. R. Hopkins, N. S. Lewis, "Detection and classification characteristics of arrays of carbon black/organic polymer composite chemiresistive vapor detectors for the nerve agent simulants dimethylmethylphosphonate and diisopropylmethylphosphonate," *Anal. Chem.* 2001, **73**, 884-892.
- ²⁴ B.S. Min, S. W. Ko, "Characterization of Segmented Block Copolyurethane Network Based on Glycidyl Azide Polymer and Polycaprolactone," *Macromolecular Research*, Vol. 15, No. 3, pp 225-233 (2007).
- ²⁵ TWAs and STELs taken from the NIOSH Pocket Guide to Chemical Hazards:
<http://www.cdc.gov/niosh/npg/>
Values for n-pentane and n-octane are used in place of isopentane and isooctane, which are not available.
- ²⁶ C.H. Arnaud, "Figuring out fracking wastewater," *Chemical and Engineering News*, 2015, (93)11, pp. 8-12.
- ²⁷ Toxicologic Assessment of Jet-Propulsion Fuel 8, Subcommittee on Jet-Propulsion Fuel 8, Committee on Toxicology, National Research Council, National Academies Press, D.C., **2003**.
- ²⁸ Angstrom Materials, Inc., Dayton, OH: <http://www.angstrommaterials.com/>
- ²⁹ Graphene Laboratories, Inc., Calverton, NY: <https://graphene-supermarket.com/Functionalized-GNPs/>
- ³⁰ Haydale Graphene Industries Plc. Ammanford, U.K.; <http://www.haydale.com/our-technology/hdplas-process/>
- ³¹ An inexpensive (~\$10) strain gage is available at www.omega.com/pptst/Bending_strain_SG.html
- ³² L.A. Currie, Nomenclature in Evaluation of Analytical Methods Including Detection and Quantification Capabilities (IUPAC Recommendations 1995) *Pure Appl. Chem.* 67 (1995) 1699-1723. $LOD = 3.29 * \sigma_0 * C / \Delta R$
- ³³ M. Pinkerova, R. Polansky, "Influence of Cross-Linking on Properties of Peva Used for Cable Sheaths," *Annals of DAAAM for 2011 & Proceedings of the 22nd International DAAAM Symposium*, Volume 22, No. 1, pp. 975-976, ISSN 1726-9679, ISBN 978-3-901509-83-4, Editor B. Katalinic, Published by DAAAM International, Vienna, Austria, EU, 2011.
- ³⁴ S. Dadbin, M. Frounchi, M. Sabet "Studies on the properties and structure of electron-beam crosslinked low-density polyethylene/poly[ethylene-co-(vinyl acetate)] blends," *Polym Int*, 54:686–691 (2005), DOI: 10.1002/pi.1750.
- ³⁵ "Thermal Properties of Elvax® Measured by Differential Scanning Calorimeter (DSC)," Dupont Technical Data Sheet, <http://www.dupont.com/products-and-services/plastics-polymers-resins/ethylene-copolymers/brands/elvax-ethylene-vinyl-acetate.html>
- ³⁶ Heuchel, M.; Al-Qaisi, L.; Kratz, K.; Nöchel, U.; Behl, M.; Lendlein, A. Thermomechanical Characterization of a Series of Crosslinked Poly[Ethylene-Co-(Vinyl Acetate)] (PEVA) Copolymers. *MRS Proceedings* **2015**, 1718, 123–130.
- ³⁷ R. Hiss, S. Hobeika, C. Lynn, and G. Strobl, "Network Stretching, Slip Processes, and Fragmentation of Crystallites during Uniaxial Drawing of Polyethylene and Related Copolymers. A Comparative Study," *Macromolecules* **1999**, 32, 4390-4403.
- ³⁸ Unpublished work: Model terms were selected from a set used in a project to model chemical concentrations based on the response of four chemical sensors, temperature and humidity (2009).